Carboxypeptidase E reduces Glioblastoma migration through modulation of motility-associated gene expression and signaling cascades

Dissertation

zur Erlangung des Grades eines
Doktors der Naturwissenschaften

der Mathematisch-Naturwissenschaftlichen Fakultät und
der Medizinischen Fakultät
der Eberhard-Karls-Universität Tübingen

vorgelegt von

Angela Armento

aus Acquaviva delle Fonti (BA), Italy

February - 2017

Tag der mündlichen Prüfung:03-05-2017.....

Dekan der Math.-Nat. Fakultät: Prof. Dr. W. Rosenstiel

Dekan der Medizinischen Fakultät: Prof. Dr. I. B. Autenrieth

1. Berichterstatter: Prof. Ulrike Naumann

2. Berichterstatter: Prof. Stefan Liebau

Prüfungskommission: Prof. Ulrike Naumann

Prof. Stephan Liebau

Prof. Robert Feil

Prof. Stephan Huber

Erklärung / Declaration:

Ich erkläre, dass ich die zur Promotion eingereichte Arbeit mit dem Titel:

„Carboxypeptidase E reduces Glioblastoma migration through modulation of motility-associated gene expression and signaling cascades“

selbständig verfasst, nur die angegebenen Quellen und Hilfsmittel benutzt und wörtlich oder inhaltlich übernommene Stellen als solche gekennzeichnet habe. Ich versichere an Eides statt, dass diese Angaben wahr sind und dass ich nichts verschwiegen habe. Mir ist bekannt, dass die falsche Abgabe einer Versicherung an Eides statt mit Freiheitsstrafe bis zu drei Jahren oder mit Geldstrafe bestraft wird.

I hereby declare that I have produced the work entitled

*"*Carboxypeptidase E reduces Glioblastoma migration through modulation of motility-associated gene expression and signaling cascades*"*

submitted for the award of a doctorate, on my own (without external help), have used only the sources and aids indicated and have marked passages included from other works, whether verbatim or in content, as such. I swear upon oath that these statements are true and that I have not concealed anything. I am aware that making a false declaration under oath is punishable by a term of imprisonment of up to three years or by a fine.

Tübingen, den 11-05-2017 Augusto Amuento

Datum / Date Unterschrift /Signature

TABLE OF CONTENTS

ABBREVIATIONS LIST

ADAMTS4	A disintegrin and metalloprotease with trombospondin motifs
AKT	protein kinase B
AMPK	adenosine monophosphate-activated protein kinase
ANGPT	angiopoietin
ARF6	ADP-ribosylation factor 6
ATP	adenosine triphosphate
ATRX	ATP-dependent helicase, X-linked
BCL-2	B-cell lymphoma 2
BCL-XL	B-cell lymphoma-extra large
BDNF	brain-derived neurotrophic factor
BIRC5	baculoviral IAP repeat containing 5, survivin
CD26	cluster of differentiation 26
CD9	tetraspanin
CDC42	cell division cycle 42
CDK4	cyclin dependent kinase 4
CDKN2A/p21	cyclin-dependent kinase inhibitor 2A
CDKN1B/p27	cyclin-dependent kinase inhibitor 1B
CMV	citomegalovirus
CNS	central nervous system
CPE	carboxypeptidase E

CRC	colorectal cancer
DNA	deoxyribonucleic acid
EBRT	external beam radiation therapy
ECM	extracellular matrix
EGFP	enhanced green fluorescent protein
EGFR	epidermal growth factor receptor
ER	endoplasmic reticulum
ERK	extracellular signal–regulated kinase
FAK	focal adhesion kinase
FAS	Fas cell surface death receptor
FDR	false discovery rate
FGF	fibroblast growth factor
GBM	glioblastoma
GLUT	glucose transporters
GRB2	growth factor receptor-bound protein 2
GSC	glioblastoma stem cells
GTP	guanosine triphosphate
H3	histone 3
HCC	hepatocellular carcinoma
HD	hystone deacetylase
HE	hematoxylin/eosin
HIF	hypoxia inducible factor
HTA	Human Transcriptome Array
IDH	isocitrate-dehydrogenase

IL	interleukin
INK4A	cyclin-dependent kinase inhibitor 2A
INS	insulin, proinsulin
IPA	Ingenuity Pathway Analyses
JAK	receptor-associated Janus kinase
LDHA	lactate dehydrogenases
LKB1	liver kinase B1
LOH	loss of heterozygosis
MAL	myelin and lymphocyte protein
MAPK	mitogen-activated protein kinase
MBP	myelin basic protein
MCT4	lactate transporters
MDM2	Double Minute 2
MGAT4A	acetyl-glucosamyl-transferase IV A
MGMT	O-6-methylguanine-DNA methyltransferase
MGST1	microsomal glutathione-s-transferase 1
MHC	major histocompatibility complex
miR	microRNA
MMP	matrix metalloproteinases
MSI1	Musashi RNA binding protein 1
Mut	mutant
NEDD9	neural precursor cell expressed, developmentally down-regulated 9
NES	nestin

NF1	neurofibromin 1
NFkB	nuclear factor kappa B
NK	natural killer
OCT4	POU class 5 homeobox 1
OLIG2	oligodendrocyte lineage transcription factor2
OPN/SPP1	secreted phosphoprotein 1
OV	oncolytic virus
PAK	p21-activated kinase
PC	prohormone convertase
PCDH17	protocadherin 17
PDGFR	platelet derived growth factor receptor
PD-L1	programmed death-ligand 1
PENK	proenkephalin
PHEOs/PGLs	pheochromocytomas/ paragangliomas
POMC	proopiomelanocortin
PPAR	peroxisome proliferator activated receptor
PPP	pentose phosphate pathway
PTEN	phosphatase and tensin homolog
RAC1	ras-related C3 botulinum toxin substrate 1
RAF	Raf-1 proto-oncogene, serine/threonine kinase
RAS	Ras proto-oncogene, GTPase
RB	retinoblastoma protein
RHOA	ras homolog family member A

RNA	ribonucleic acid
RSP	regulated secretory pathway
SDF	stromal cell derived factor
SMAD2	mothers against DPP homolog 2
SNAIL1	snail family transcriptional repressor 1
SNAIL2	snail family transcriptional repressor 2
SOS	SOS Ras/Rac guanine nucleotide exchange factor
SOX2	SRY-box 2
STAT3	signal transducer and activator of transcription 3
STC1	stanniocalcin-1
TGF	transforming growth factor
TGN	trans-Golgi network
TIMP	tissue inhibitor of metalloproteases
TMZ	temozolomide
TP53	tumor protein p53
TRAIL	TNF-related apoptosis inducing ligand
TWIST	twist family bHLH transcription factor
VEGF	vascular endothelial growth factor
WHO	World Health Organization
WNT	wingless-type MMTV integration site family
Wt	wild-type
XIAP	X-linked inhibitor of apoptosis

YB-1	Y-box binding protein 1
ZEB	zinc finger E-box binding homeobox
ZFPM2	zinc finger protein, FOG family member 2

1. ABSTRACT

Glioblastoma (GBM) is the most common and most malignant brain tumor in humans. The prognosis is poor since GBM is highly-resistant to therapy and possesses a strong migratory and invasive potential, making complete surgical resection impossible. Previous work demonstrated that Carboxypeptidase E (CPE), originally identified as a neuropeptide processing enzyme, is secreted by a subcohort of malignant glioma and, if overexpressed in glioma cells, exerts anti-migratory, but pro-proliferative activity, suggesting that CPE might be a ‘‘Go or Grow’’ switch factor. Here we describe CPE mainly as an anti-migratory protein in glioma cells and we aim in deciphering the mechanism by which CPE modulates glioma cell behavior. Using transcriptome analyses, followed by Ingenuity Pathway Analyses (IPA) and investigation of several signaling cascades, we found that in CPE-overexpressing cells a variety of motility-associated mRNAs and miRNAs were differentially regulated and connected to motility-associated networks including FAK, PAK, CDC42, integrin, STAT3, TGF-β as well as ERK1/2. In particular

SNAI2/SLUG, a transcription factor known to induce tumor cell motility and metastasis, was downregulated. Matrix-Metallo-Proteases (MMP) as well as MMP-activity inducing factors, all necessary for glioma cell invasion, were reduced in CPE-overexpressing cells. SNAI2/SLUG expression was regulated via ERK1/2 since inhibition of ERK1/2 activation abolished CPE-mediated SLUG downregulation and reduction of cell migration. Moreover, we showed a synergistic effect of CPE overexpression in combination with standard glioma therapy (Temozolomide and radiation) in the clonogenic survival of GBM cells. *In vivo*, the anti-migratory capacity of CPE translated in prolonged survival of mice bearing CPE-overexpressing tumors. These data help to understand the role of migration in glioma aggressiveness and how CPE is involved in this process.

2. INTRODUCTION

2.1 GLIOBLASTOMA

2.1.1 General features

Gliomas are a common adult central nervous system (CNS) tumor and they account for the 77% of primary brain tumors diagnosed every year worldwide, which are more than 250000 new cases [1]. Nearly 60% of high-grade gliomas are glioblastoma (GBM) and incidence has been increasing in the last decades up to 3,5 new cases of GBM per 100000 inhabitants in western countries every year [2]. GBM is clearly the most frequent, but unfortunately also the most aggressive and malignant brain tumor. Symptomatology in glioma patients is distinctly different from other cancer patients because of the neurological symptoms like paresis, visual-perception deficits, sensory loss, cognitive deficits or seizures, and in some cases changes in personality and behavior have been reported [3, 4]. GBM are called *glioblastoma multiforme* due to the high heterogeneity of cells in the tumor and among different GBMs. Because of that, classification is in constant evolution due to the discovery of new mutations and refined diagnostic tools, especially for molecular

features. The WHO (World Health Organization) recently felt the need to update the previous glioma classification from 2007 [5]. Former classification was mainly based on histological characteristics of the tumor and as a result 4 different grades were individuated (I-IV), with the lower grades supposed to be less aggressive and have a better outcome and higher grades to have a poor prognosis. The updates on glioma classification will be presented in detail later. GBM presents characteristics which makes it the most malignant brain tumor. Indeed, because of the highly infiltrative growth, complete surgical resection is impossible and recurrence is inevitable. If untreated, GBM leads to death in 3 to 6 months, and even providing the best therapy options, which includes irradiation and chemotherapy after surgery, median patient survival increases to only 15 months [6]. Despite the efforts in the last decades in GBM research, alternative treatment options or adjuvants applied to standard therapy are urgently needed.

2.1.2 Glioma classification

The World Health Organization (WHO) redefined the classification of tumors of the central nervous system in 2016 [7], integrating the histological criteria used in the

previous WHO classification 2007 [5] with more updated molecular parameters.

The class of brain tumor relevant for this work is the diffuse glioma (Table 2.1.1), which includes all diffusely infiltrating gliomas, whether they developed from cells of astrocytic or oligodendroglial origin. They are divided in the WHO grade II and grade III astrocytic tumors, the grade II and III oligodendrogliomas and the grade IV GBM. The higher grade indicates a more malignant and aggressive phenotype, as in the former classification. They are grouped according to their growth pattern and behavior and the subclasses are based on the shared genetic driver mutations in the *isocitrate-dehydrogenase* (IDH)1 and IDH2 genes. In the past the status of these genes, mutated (mut) or wild-type (wt), was mainly used in diagnosis to define whether a GBM was a primary *de novo* tumor (IDH wt) or secondary (IDH mut), arising from a lower grade glioma [8]. Moreover a third class of GBM is called GBM NOS in case the status of IDH genes cannot be defined. An additional variant of GBM, called epithelioid glioblastoma, has been introduced. It joins giant cell glioblastoma and gliosarcoma under the class of IDH-wildtype GBM. Other key mutations or genetic alterations necessary for the classification of diffuse gliomas are the 1p/19q codeletion,

which is prognostically favourable, and K27M mutations in the *histone 3* (H3) gene, found in midline diffuse glioma [7].

Diffuse astrocytic and oligodendroglial tumours	
Diffuse astrocytoma, IDH-mutant	9400/3
Gemistocytic astrocytoma, IDH-mutant	9411/3
Diffuse astrocytoma, IDH-wildtype	*9400/3*
Diffuse astrocytoma, NOS	9400/3
Anaplastic astrocytoma, IDH-mutant	9401/3
Anaplastic astrocytoma, IDH-wildtype	*9401/3*
Anaplastic astrocytoma, NOS	9401/3
Glioblastoma, IDH-wildtype	9440/3
Giant cell glioblastoma	9441/3
Gliosarcoma	9442/3
Epithelioid glioblastoma	*9440/3*
Glioblastoma, IDH-mutant	9445/3*
Glioblastoma, NOS	9440/3
Diffuse midline glioma, H3 K27M–mutant	9385/3*
Oligodendroglioma, IDH-mutant and 1p/19q-codeleted	9450/3
Oligodendroglioma, NOS	9450/3
Anaplastic oligodendroglioma, IDH-mutant and 1p/19q-codeleted	9451/3
Anaplastic oligodendroglioma, NOS	*9451/3*
Oligoastrocytoma, NOS	*9382/3*
Anaplastic oligoastrocytoma, NOS	*9382/3*

Table 2.1.1 2016 WHO classification of diffuse glioma. Table depicted from [7], representing the 2016 WHO classification of tumors of the CNS.

Nevertheless the histological features of diffuse gliomas still play an important role in their classification. In particular GBM are characterized by hypercellularity, pronounced angiogenesis, high proliferation rate, infiltrative growth, nuclear atypia and central necrosis (Figure 2.1.1). A simplified schema for diffuse glioma classification and grading is shown in Figure 2.1.2.

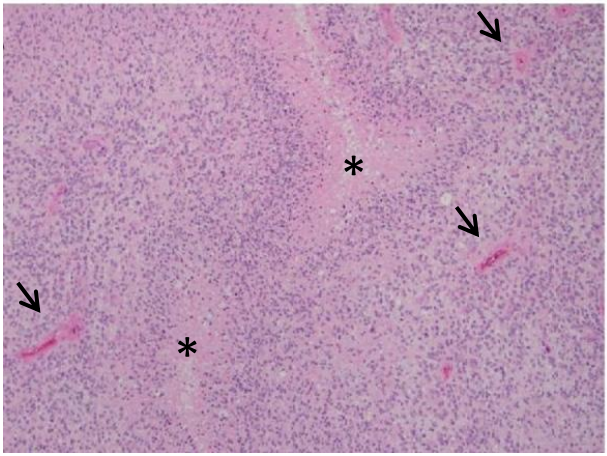

Figure 2.1.1 Hematoxylin/eosin (HE) stain of a section of a GBM [9].
Arrows indicate blood vessels, asterisks indicate necrotic areas surrounded by pseudopalisading cells.

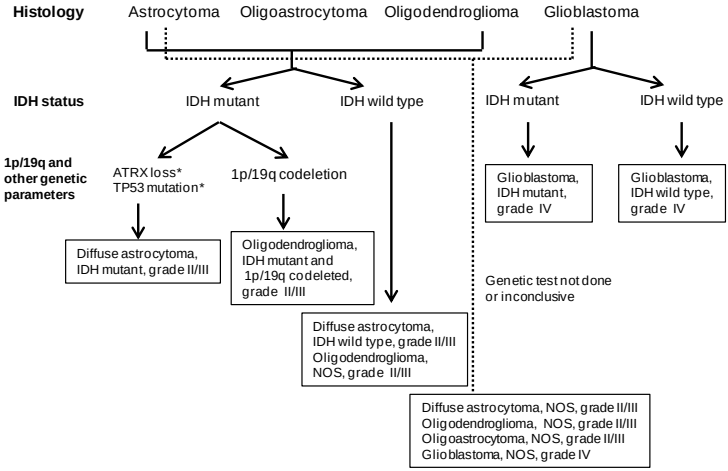

Figure 2.1.2 Schematic representation of diffuse glioma classification. Grades indicate malignancy,
*: characteristic, but not required for diagnosis, revisited from [7].

In parallel with the update in CNS tumor classification, several studies have been performed in the last years to divide gliomas, especially GBM, in different subtypes according to common mutations and phenotypes. The most important studies were performed by Philips [10] and Verhaak [11] and four subtypes have been specified: proneural, classical, mesenchymal and neural (Figure 2.1.3).

The proneural (PN) subtype is defined by a better prognosis and expression of genes associated with healthy brain tissue and neurogenesis. The other subtypes differ from the PN subtype primarily because of the poor prognosis and a shorter patient survival. Tumors belonging to the mesenchymal (Mes) subtype exhibit indications of increased migration, angiogenesis and enhanced microvascular proliferation. The proliferative (Prolif) subtype, as indicated by its name, is characterized by a high proliferation rate, revealed by a high percentage of tumor cells active in cell division. This last subtype is then divided in neural and classical subtypes, because of the presence in the neural group signature of genes differentially expressed by neurons.

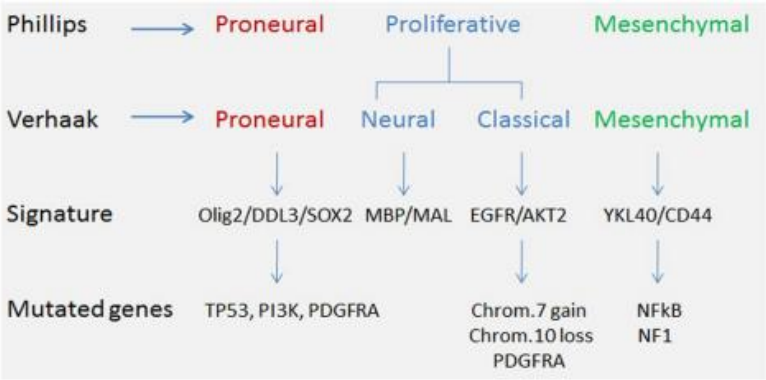

Figure 2.1.3 Transcriptional subtypes of GBM based on the classification defined by Phillips and Verhaak [12].

2.1.3 Molecular mechanisms involved in GBM malignancy

The main reason for the high malignancy of GBM is the inevitable recurrence due to the highly infiltrative phenotype and the impossibility to remove all the tumor cells completely during surgical resection. Besides that, GBM malignancy is also accompanied by other pro-tumorigenic aberration that enhance cell growth, help to overcome cell death or anti-tumor immune responses or that leads to therapy resistance.

2.1.3.1 Proliferation and cell cycle

As proved by histology, GBM cells present a high proliferation rate which is often caused by mutations or genetic alterations leading to uncontrolled proliferation and malfunctioning of the cell cycle key check-points.

About 50% of GBM present perturbation of the *epidermal growth factor receptor* (EGFR), represented by an amplification or the presence of a constitutive active variant (EGFR vIII). The latter is a product of a deletion of exon2-7 in the EGFR gene, leading to the expression of a truncated version of EGFR, lacking a part of the extra cellular domain. In both cases activation of pro-proliferative signaling cascades like the *mitogen-activated*

protein kinase (MAPK)/*extracellular signal-regulated kinase* (ERK) pathway occurs [13]. The classical activation of the EGFR signaling cascade starts with the extracellular ligand EGF, binding to its receptor on the cell surface. This interaction leads to an auto-phosphorylation of EGFR, and via interaction with scaffold proteins like *growth factor receptor-bound protein 2* (GRB2) and *SOS Ras/Rac guanine nucleotide exchange factor* (SOS), allows the activation of the small GTP binding protein (RAS), subsequently inducing the phosphorylation and activation of a cascade of kinases: RAF/MEKK/MEK/ERK. Ultimately, this activation leads to the activation of transcription factors and finally alters gene expression of cell cycle control genes [14].

Other common mutations in GBM which lead to an uncontrolled cell cycle are inactivating mutations of tumor suppressors such as *tumor protein p53* (TP53) or *retinoblastoma-protein* (RB), or mutations of their regulators. One example is the gene INK4A, which encodes two different proteins due to the presence of alternative splicing sites, *cyclin dependent kinase inhibitor 2A* (CDKN2A-p14^{ARF} and CDKN2A-p16^{INK4a}). Binding of the first one with *double minute 2* (MDM2) leads to correct activation of p53. On the other hand, CDKN2A-p16^{INK4a}

negatively regulates *cyclin dependent kinase 4* (CDK4), which controls the activity of RB. Therefore a simultaneous inactivation of CDKN2A-p14^{ARF} and CDKN2A-p16^{INK4a} causes deregulation of both RB and p53 pathways [15].

Another tumor suppressor involved in GBM gliomagenesis is *phosphatase and tensin homologue deleted on chromosome 10* (PTEN), which negatively regulates *protein kinase B* (AKT) pathway. Loss of heterozygosis (LOH) at the 10q23.3 locus or gene mutations (15% to 40%) leads to the loss of function of PTEN, a constitutively activated signaling pathway and, besides other pro-tumorigenic effects, to uncontrolled cell proliferation [15].

2.1.3.2 Apoptosis and cell death

Many chemotherapy approaches as well as tumor irradiation used for GBM treatment are ineffective due to the fact that GBM cells developed several mechanisms to overcome cell death. For example, a variety of proteins that are necessary for the induction of apoptosis by extrinsic or intrinsic stimuli, are differentially expressed in GBM. Expression of death receptor molecules such as *Fas cell surface death receptor* (FAS) or *TNF-related apoptosis inducing ligand* (TRAIL) are often downregulated while

the expression of decoy receptors that compete for death ligand binding can be upregulated. Moreover, caspase activation might be blocked by loss of function mutations in these protein or by overexpression of anti-apoptotic proteins like *B-cell lymphoma 2* (BCL-2), *B-cell lymphoma-extra large* (BCL-XL), *baculoviral IAP repeat containing 5* (BIRC5, survivin) or *X-linked inhibitor of apoptosis* (XIAP) (for review see [16]).

2.1.3.3 Migration and invasion

As already specified above, GBM is characterized by a strong infiltrative growth, which is the result of the activation of pro-migratory and pro-invasive pathways, often accompanied by the rearrangement of the cytoskeleton. Different components of the plasma membrane, like integrins, can also regulate motility-associated signaling cascades, and altered integrin expression can be correlated to cancer progression and malignancy. Integrins are proteins that anchor cells to the extracellular matrix (ECM), and integrin subtype expression is different in malignant versus non-neoplastic cells. For example, integrin $\alpha_v\beta_3$ is abundantly expressed in high grade brain tumors [17].

Focal adhesion kinase (FAK) is a non-receptor tyrosine kinase involved in signal transduction pathways activated by integrin-mediated cell adhesion and by growth factor receptors [18]. It modulates several processes, including migration and invasion. Perturbation of FAK activity impairs GBM cell migration [19].

The small Rho-GTPases (*ras homolog family* member A RHOA, *ras-related C3 botulinum toxin substrate 1* RAC1, *cell division cycle 42* CDC42) and their effectors, including *p21 activated kinase* 1 (PAK), play an important role in GBM migration and invasion by modulting filopodia and actin stress fiber formation in glioma cells, thus leading to a more migratory and invasive phenotype [20].

Other migration-associated pathways involve the *signal transducer and activator of transcription 3* (STAT3) and the *transforming growth factor β* (TGFβ). In response to growth factors or cytokines, STAT3 is phosphorylated by *receptor-associated Janus kinase* (JAK). This event leads to STAT3 dimerization and its translocation into the nucleus where it can act as a transcription factor [21]. STAT3 activation is associated with a more malignant glioma phenotype and poor clinical outcome [22]. Moreover, STAT3 silencing inhibits glioma single cell

infiltration and reduces the expression of many motility-associated genes [23].

TGFβ binds to its specific receptor (TGFβRI) leading to the recruitment and phosphorylation of TGFβRII, which can in turn phosphorylates *mothers against DPP homolog 2/3* (SMAD2/3). Phosphorylated SMAD2/3 form a heterodimer with SMAD4. This complex shifts into the nucleus and modulates genes transcription [24]. TGFβ promotes, among others, activation of matrix metalloproteinases (MMPs) [25], necessary for ECM remodeling during tumor cell invasion. In particular, overexpression of MMP-2 and MMP-9 correlates with high grade glioma [26].

The exact mechanisms by which tumor cells invade the surrounding healthy brain tissue are still under investigation. Transcription factors like *zinc finger E-box binding homeobox* (ZEB1/2), *twist family bHLH transcription factor* (TWIST), *snail family transcriptional repressor 1* (SNAIL1/SNAIL) and *snail family transcriptional repressor 2* (SNAIL2/SLUG) lead to changes in the expression of cell surface proteins such as cadherins, vimentin and others, subsequently regulating cell invasive processes in many tumors, and also in gliomas. Silencing of SNAIL1 reduces proliferation, invasion and migration of GBM cells [27], and SLUG

expression has been found to be higher in GBM specimens and correlates to a more invasive phenotype and high grade GBM. Moreover SLUG promotes invasion and angiogenesis in *in vitro* and *in vivo* models [28]. Higher ZEB2 expression in human GBM samples correlates with fast tumor progression in GBM patients [29].

Interestingly, many of these motility pathways and mechanisms are interconnected. As example, TGFβ promotes glioma cell migration via up-regulation of integrin $\alpha_v\beta_3$ [30] and both STAT3 and TGFβ modulate the expression of SLUG, SNAIL and TWIST [31, 32].

2.1.3.4 Hypoxia, neoangiogenesis and metabolic changes

During tumor growth, a part of the glioma cells located in the inner portion of the tumor can face hypoxia and nutrients starvation. Therefore glioma cells developed strategies to overcome this adverse situation. First of all, around the necrosic and hypoxic regions of GBM pseudopalisading cells become prominent. These glioma cells change their phenotype to a more migratory phenotype in an attempt to leave the hypoxic region and reach the closest blood vessel for oxygen and nutrient supply [33]. During oxygen deprivation, *hypoxia-inducible*

factor 1 (HIF1α) is stabilized and induces the expression of several genes like *vascular endothelial growth factor* (VEGF), *fibroblast growth factor* (FGF), *stromal cell derived factor* (SDF) or *angiopoietin* (ANGPT) that trigger neoangiogenic processes [34].

Glioma cells as well as almost all tumor cells use more anaerobic glycolysis to provide energy in place of oxidative phosphorylation, the so called Warburg effect. By this, tumor cells become more resistant to hypoxia. In addition, the expression of glucose transporters and the glucose uptake is increased and lactate production is elevated in tumor cells. The changes in metabolic activity as well as hypoxic conditions induce tumor cell migration and invasion, also of glioma cells (for review see [35]).

2.1.3.5 Immunosuppression

Glioma cells mainly escape the attack of the immune system and for this they use different mechanisms. Glioma secreted TGF-β, besides its pro-migratory function, is a potent immune-suppressive cytokine. It blocks T-cell activation and expansion, inhibits natural killer (NK) cells activity and, in an autocrine fashion, leads to the camouflage of glioma cells by downregulation of *major histocompatibility complex* (MHC) protein expression or by

shading of NK-cell ligands expressed on the cell surface. Moreover, GBM cells express *programmed death-ligand 1* (PD-L1), which binds to the T cell exhaustion receptor PD-1, this way inhibiting the activation of tumor infiltrating T cells (for review see [36]).

2.1.3.6 Glioma stem cells

As mentioned above, GBM cells show great heterogeneity in mutations as well as in their behavior and can change their behavior not only by genetic or epigenetic alterations, but also reversibly during environmental alterations in the surrounding tumor micro-milieu. In this regard it has been shown that a small population of glioma cells in the tumor harbor stem cell characteristics, are highly therapy resistant and are postulated to be responsive for recurrence of this disease (for review see [37]). GBM stem cells (GSC) are defined as cells sharing normal neural progenitor features including the expression of neural stem cell markers [e.g. *Musashi RNA binding protein 1* (MSI1), *nestin (*NES), *SRY-box 2* (SOX2), *POU class 5 homeobox 1 (*OCT4)], having the capacity for self-renewal and neurospheres formation.

2.1.4 Treatment options for glioma

The current standard therapy for GBM is surgical resection of the tumor followed by radiochemotherapy, known as the STUPP regime [6]. The level of resection is case-specific depending on tumor size, shape and location. The bigger and more accurate the resection, the greater is the chance of prolonged survival.

Radiation therapy causes severe DNA damages leading to apoptosis-induced cell death. Radiation therapy can be performed as external beam radiation therapy (EBRT) or radiosurgically, for example with gammaknife techniques. The standard chemotherapy is Temozolomide (TMZ), an alkylating agent that methylates purines in DNA. The success of the treatment is highly dependent on the genetic background of the tumor cells, in particular the methylation state of the *O-6-methylguanine-DNA methyltransferase* (MGMT) promoter. MGMT mediates DNA mismatch repair after TMZ-induced damage, therefore the treatment is more effective when the MGMT promoter is methylated. Indeed, patient survival rates are higher in patients with MGMT promoter methylation (21.5 versus 15.3 months) [38]. Nevertheless, overall survival is still short and novel therapies are needed.

One new class of therapeutic agents are monoclonal antibodies that recognize cell surface receptors or ligands, this way disrupting the receptor-ligand interaction and preventing the activation of tumor signaling cascades. Examples are Avastin /Bevazizumab, an antibody neutralizing the function of VEGF, postulated to inhibit neoangiogenesis [39] or Erbistux/Cetuximab, an EGFR-specific monoclonal antibody [40], that has been used in tumor therapy due of the high frequency of EGFR mutations or amplification in GBM. Some difficulties have been observed in this kind of therapy, such as the lack of these antibodies to cross the blood-brain barrier, or systemic toxicity. Other attempts in immunotherapy have been made using vaccine based drugs that target patient specific tumor antigens or commonly overexpressed antigens in GBM. Besides this several other strategies are under observation that should improve the anti-tumoral immune response (for review see [41]). Another approachto treat GBM is based on the use of oncolytic viruses (OV). OV are genetically manipulated to target and to kill cancer cells whilst leaving non-neoplastic cells unaffected. This is achieved by manipulating the OV in a way that makes virus replication possible only in the presence of certain cancer specific or proteins

overexpressed in tumor cells such as *Y-box binding protein 1* (YB-1), EGFRvIII, *platelet derived growth factor receptor* (PDGFR) or *interleukin 13 receptor* (IL-13R). This approach could be also useful to target the population of GSC that are mainly resistant to most available therapies (for review see [42]).

With the most updated diagnostic tools, involving the analyses of genetic and molecular profiles of each single GBM, the idea of personalized medicine is becoming more and more feasible and promising [43].

2.2 “GROW OR GO” HYPOTHESIS

The “Grow or Go” hypothesis (Figure 2.2.1) is based on the assumption that a cell is not able to proliferate and migrate at the same time, mostly because the two mechanism share the same cell component, the cytoskeleton, and both requires great energy consumption. This phenomenon was first observed in astrocytoma cells in 1996, where it was discovered that proliferation and migration were mutually exclusive in time. [44]. The “Grow or Go” principle might be also of therapeutic importance since it is suggested to be involved in the progression from benign neoplasms (uncontrolled proliferation) to malignant invasive tumors (high migration) [45]. This behavior has been largely studied in GBM, and even a mathematical model to explain the process have been created [46].

It has been shown that the switch from migration to proliferation and vice versa can be caused by changes in the microenvironment. For example hypoxia or nutrient depletion prompts a tumor cell to “Go”. Eventually the migrated cell will re-settle in a new niche providing optimal conditions and then adapts itself to “Grow” again [45]. Indeed, under hypoxic conditions glioma cells change their phenotype to a more pro-migratory one. This change

is mediated by metabolic adaptation, and in particular the pentose phosphate pathway (PPP) has been demonstrated to be prominently used during proliferation and cell division whereas glycolysis is the prominent energy source during migration [47]. But also changes in cell volume, cytoskeleton dynamics, extracellular matrix composition influence the “Grow or Go” behavior of glioma cells [45]. Moreover, ionizing irradiation, an essential therapy in GBM treatment, promotes the switch to the ”Go” phenotype in glioma cells [48] with a clear influence on the success of the treatment. Besides the physiological inducers, other molecules like miRNAs that are involved in decision of a cell to “Go or Grow” have been identified so far. In response to metabolic stress, mir-451 modulates the *liver kinase B1* (LKB1)/ *adenosine monophosphate-activated protein kinase* (AMPK) pathway. miR-451 levels are high during glucose rich conditions and promote proliferation, while miR-451 levels are reduced during glucose deprivation, paralleled by increased cell migration, at the expenses of proliferation. In GBM patients elevated miR-451 expression is associated with a shorter survival [49]. Another miRNA, highly expressed in glioma cells, is mir-9. It regulates the “Grow or Go” by inhibiting proliferation and promoting migration [50].

Carboxypetidase E (CPE), the protein of interest of this work, has been described to have a pro-proliferative but anti-migratory role in GBM cells, therefore contributing in the “Grow or Go” behavior of glioma cells [51].

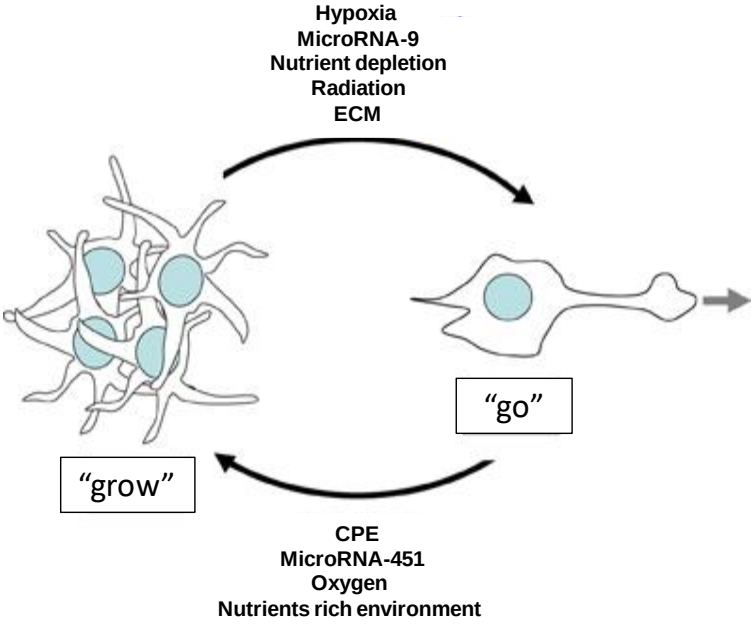

Figure 2.2.1 Schematic representation of the "Grow or Go" hypothesis. Revisited from [48].

2.3 CARBOXYPEPTIDASE E

Carboxypeptidase E (CPE) was first discovered in 1982 as an enkephalin convertase, belonging to a family of enzymes that are responsible for removing basic residues from pro-peptides [52, 53]. CPE was found to be responsible for cleaving the C-terminal basic residues of pro-peptides or neuropeptides in endocrine cells and neurons. The importance of CPE in the endocrine system became even more visible after in $CPE^{fat/fat}$ mice a mutation in the CPE gene was found that induces obesity, diabetes and infertility [54].

2.3.1 CPE gene, protein structure and activity

CPE belongs to M14-like superfamily of enzymes, a group of metallo-carboxypeptidases that cleave polypeptides at a single C-terminal amino acid, have a recognition site at C-terminal and contain a Zn^{2+} binding site [55]. In particular, CPE belongs to carboxypeptidase B-like (CPB-like) enzymes given the fact that it cleaves at basic residues (lysine or arginine). There are about 23 genes encoding for Zn^{2+}-carboxypeptidases and a comparison between CPE and CPA/B enzymes shows a very little conservation except for the Zn^{2+}-carboxypeptidase domain indicating that these proteins diverged early in evolution [56].

Interestingly, the similarity between CPE in different species is really high, highlighting the importance of this protein in early evolution. For the goal of this thesis, it is important to know that rat and human CPE are highly similar and present a very similar structure. CPE is obviously localized in neuropeptides-rich area of the brain and in endocrine tissues, such as stomach, colon, oviduct, salivary glands, pancreas and adrenal medulla [57].

CPE genes contains nine exons [58] and alternative spliced transcripts have been identified [59](Figure 2.3.1).

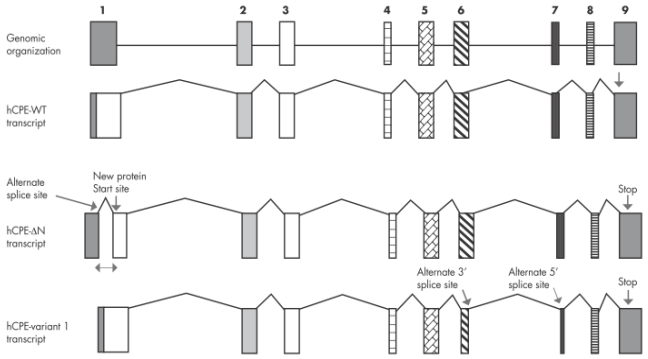

Figure 2.3.1 Representation of CPE gene and splicing variants [57]

One variant encodes for a truncated version of CPE (ΔN-CPE) which lacks a 98 amino-acids N-terminal region due to the presence of an alternative splicing site on the first exon. This version has been found to be common and highly present in metastatic tumors, for example in breast cancer [59].

CPE variant 1 is alternatively spliced at exon 6, this results into an 18 amino acid deletion leading to an enzymatically inactive protein and the absence of a functional signal peptide necessary for endoplasmic reticulum (ER) translocation. Therefore this variant is more likely to be secreted in the extracellular space [57].

The full-length version of CPE is a 476 amino acids protein (Figure 2.3.2), containing a 25 amino acid signal peptide which directs pro-CPE to the ER. pro-CPE is further processed in the Golgi-Apparatus where the 17 amino acids long signal peptide is removed and a mature form of CPE is formed, ready to exerts its function. Moreover, CPE presents two putative glycosylation sites at Asn_{139} and Asn_{390} [60] and presents several domains (Figure 2.3.2): (i) the enzymatic active site including the Zn^{2+} binding domain, (ii) a prohormone sorting signal binding site, (iii) a transmembrane domain and (iv) a cytoplasmic tail.

The mature form of CPE can be further processed at the C-terminus (Arg_{455}-Lys_{456}) to form a soluble form (50 kDa), which is smaller than the membrane-associated form (53 kDa) and is also more active [61].

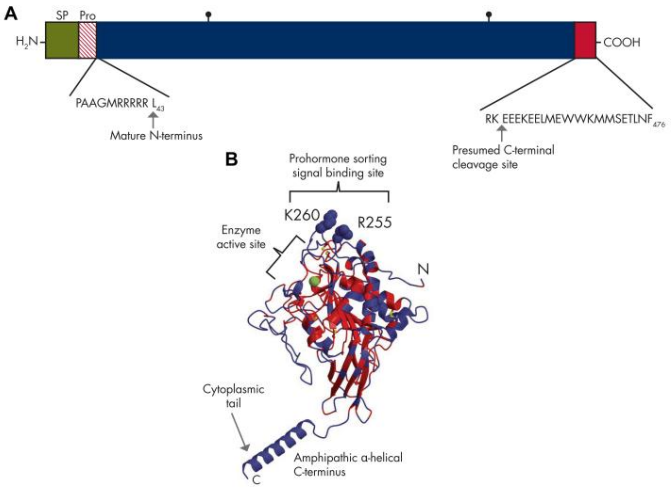

Figure 2.3.2 CPE model and structure [57]
A Schematic representation of CPE. **B** Molecular structure model of CPE.

2.3.2 CPE in prohormone sorting/processing and vesicles transport

Most cells present a constitutive secretory pathway to maintain cell survival, differentiation or growth. Neurons and endocrine cells need a tightly regulated secretory pathway (RSP) to modulate hormone and neuropeptide secretion in order to maintain the homeostasis of the organism. CPE is a very important protein involved in different steps of this process, as described in Figure 2.3.3.

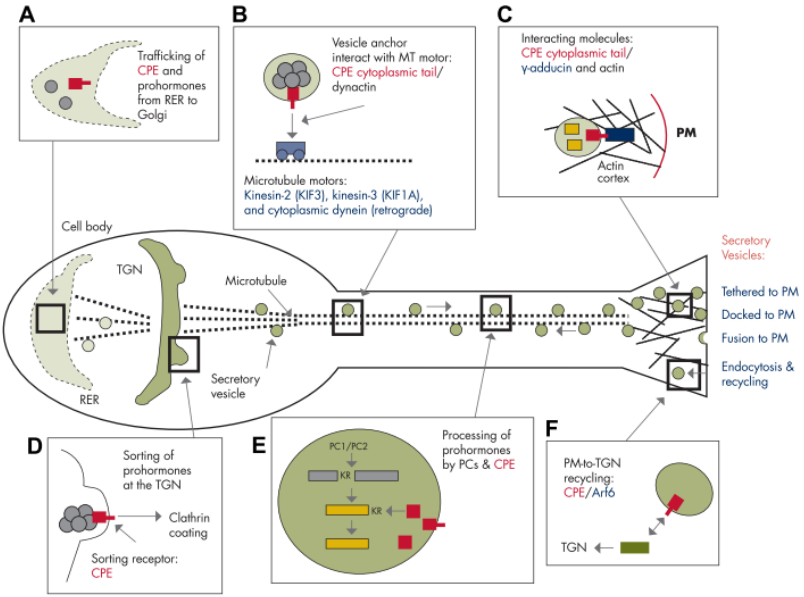

Figure 2.3.3 Trafficking of CPE in regulated secretory pathway [57].

A CPE and pro-hormones are packed into vesicles from the ER. **B** The cytoplasmic tail of CPE binds dynactin and the microtubules. **C** The vesicles are addressed to the plasma membrane. **D** CPE acts as a sorting receptor. **E** Processing of prohormones by prohormone convertases (PCs) and CPE. **F** Recycling of CPE by *ADP-ribosylation factor 6* (ARF6) recruitment.

Pro-hormones and pro-peptides are synthesized at the rough ER and are transported to the Golgi apparatus in order to reach the trans-Golgi Network (TGN) together

with the processing enzymes. At the TGN the processing enzymes, including CPE, and their substrates are packed into vesicles for regulated secretion [62]. It is fundamental that the pro-hormones or pro-peptides are sorted together with their correct processing enzymes. One mechanism proposed is aggregation as a concentration step [63] but this is not enough to explain the directionality of the RSP. CPE presents a pro-hormone sorting signal binding site (Arg_{255} and Lys_{260}), necessary for recognizing motifs common for *proopiomelanocortin* (POMC), *proinsulin* (INS), pro-*brain-derived neurotrophic factor* (pro-BDNF) and *proenkephalin* (PENK) [62, 64, 65]. The role of CPE as a sorting receptor has been described in different models and it is the membrane bound form of CPE that is responsible for this function. During vesicle transport to the plasma membrane, the granules undergo maturation, including acidification. This step is really important since the enzymatic activity of CPE reaches an optimum at pH 5-6 and becomes inactive at pH 7.4 [66]. After cleavage, mature hormones and neuropeptides are released into the extracellular space by exocytosis and transmembrane CPE is recycled back to TGN via recruitment and interaction with ARF6, a small cytoplasmic GTPase [67].

2.3.3 CPE and neuroprotection

Besides its role in pro-hormone sorting and processing, CPE has been found to be involved in the response to different stress stimuli and neuroprotection. Neurons of the hippocampus or cortex upregulate CPE after ischemic stress, leading to neuronal survival. On the contrary, in models lacking CPE these neurons become apoptotic after ischemic episodes [68, 69].

CPE has been described as a neurotrophic factor. *In vitro* a secreted, non-enzymatic form of CPE protects rat hippocampal neurons against oxidative stress caused by H_2O_2. This protection activity is mediated by activation of the ERK1/2 and AKT pathways, this leading to the upregulation of the anti-apoptotic protein BCL-2 and inhibition of caspase-3 [70]. Moreover, also ΔN-CPE has been found to be transiently expressed in early development and, in this time frame, to protect embryonic neurons against glutamate-induced neurotoxicity. ΔN-CPE is found in the nucleus and here can mediate the overexpression of FGF2, which in turn can be secreted and subsequently activates ERK1/2 and AKT, also leading to enhanced BCL-2 expression [71].

CPE has been linked to protection to apoptosis and cell survival not only in the brain, but also in other endocrine

tissues. There is a correlation between CPE and palmitate-induced ER stress in pancreatic β-cells. Increased Ca^{2+} influx during palmitate-induced apoptosis is necessary for the degradation of CPE, probably given the fact that Ca^{2+} high levels strongly affect CPE stability. Interestingly, CPE overexpression can partially rescue β-cells from the apoptotic process caused by palmitate toxicity [72].

The role of CPE in survival and apoptosis is still under investigation, considering a possible involvement in age related neurodegenerative disease such as Alzheimer or Parkinson disease.

2.3.4 CPE and cancer

The role of CPE in endocrine and non-endocrine tumors has been highly investigated. Concerning non-endocrine tumors, it is interesting to notice that CPE is not usually expressed in the healthy tissues, while it has been shown to be expressed (or even highly expressed) in cancers derived from the same tissues. CPE is expressed in liver [73] and breast cancer cells [74], but not in their respective normal tissues. Moreover, CPE is not expressed in cervical or colon tissue, but during cancerogenesis its level is increased in cervical and colon cancer cells [75]. Even though CPE is expressed in the brain, two independent studies have shown that CPE is highly expressed in glioma biopsies compared to normal brain tissue [76]. Microarray expression analyses of tumor biopsies indicate that metastatic tumors present higher levels of CPE mRNA compared to healthy tissue or benign tumors [75] drawing CPE as a biomarker for metastatic tumors. But since most of the studies are performed at mRNA level is not clear which variant of CPE, namely the pro-tumorigenic ΔN-CPE variant, is expressed in those tumors. For several tumor entities, ΔN-CPE variant has been found to be correlated to a high metastatic phenotype and poorer prognosis. Overexpression of ΔN-CPE predicts poor

prognosis in colorectal cancer patients [77], CPE-ΔN was found highly expressed in human hepatocellular carcinoma HCC and breast metastatic tumor cell lines, and silencing of ΔN-CPE was able to reduce metastasis in mice. Moreover, high ΔN-CPE mRNA copy numbers were found in biopsies of pheochromocytomas/paragangliomas (PHEOs/PGLs) and correlate with the prediction of metastasis and recurrence in these patients [59]. In HCC cells ΔN-CPE is able to translocate into the nucleus and there interacts with *histone deacetylase* (HD) 1/2. ΔN-CPE upregulates the *neural precursor cell expressed developmentally downregulated gene 9* (NEDD9) and enhances invasion and migration of melanoma cell lines [59].

The involvement of full-lengh CPE in different cancers is still under investigation. The function of this CPE variant in tumor cells is diverse and modulates cellular processes and cascades involved in tumor progression that can be or not be dependent on its enzymatic activity. The function of CPE in cancer is therefore controversially discussed. In HCC cells CPE, by activation of ERK1/2, can induce the expression of pro-survival factors such as BCL-2. Otherwise, CPE reduces migration and invasion of fibrosarcoma [78] and glioma cell [51]. In colorectal cancer

cell lines CPE is overexpressed and induces proliferation and cell growth through downregulation of p21 and p27 and upregulation of cyclinD1 [79]. CPE can also interfere with further signaling cascades involved in cancer progression, such as the β-catenin pathway. It has recently shown that CPE inhibits the secretion and activity of *wingless-type MMTV integration site family* (WNT) 3a, forming non-soluble aggregates with Wnt3a [80].

In GBM, CPE has been described as a "Grow or Go" factor. In particular a secreted version of CPE was able to reduce migration and induce proliferation of glioma cells, independently from its enzymatic activity [51]. Controversial results have been recently published suggesting that CPE can promote proliferation, tumor growth and metastasis, but also reduces tumor cell migration and invasion. However, it is not clear whether these effects (or which effects) are induced by ΔN-CPE or by its full length counterpart [81].

2.4 AIM OF THE STUDY

The present thesis project aims to examine the role of a secreted version of CPE (sCPE) in the "Grow or Go" phenomena in glioma cells, focusing on its anti-migratory effects previously shown in our lab. In this regard, changes in the expression of motility-associated genes will be analyzed as well as signaling cascades that are modulated by CPE will be identified.

The pro-survival and pro-proliferative role of CPE has been investigated in other cancer entities, like HCC or colorectal cancer (CRC). The ERK1/2 and AKT pathways have been proposed to be mediators of CPE-associated effects in these cells, resulting in the regulation, among others, of anti-apoptotic BCL-2 as well as of the cell cycle regulating proteins $p21^{WAF1}$ or $p27^{KIP-1}$. However, the detailed mechanisms by which CPE modulates glioma cells motility have not been investigated so far. In the present study using mRNA microarray chip technology we investigate CPE-mediated changes in gene expression, especially of motility-associated genes as well as the functional impact of differentially regulated genes in GBM cells. We further aim to identify the signaling cascades by which CPE transmits its anti-migratory effects in GBM cells. Moreover, putative receptors or binding proteins by which

sCPE transmits its anti-migratory properties form the extracellular space into glioma cells, focusing on the identification of secreted, membrane-bound or intracellular CPE-binding partners, should be examined.

Due to its anti-migratory function in GBM cells, CPE might be an interesting candidate gene for a novel GBM therapy approach. Overexpression of CPE in cancer cells might reduce the invasive growth of the tumor, pushing it into a more solid one, by this making it better operable. Therefore we additionally analyzed whether CPE might enhance the effects of GBM standard therapy approaches *in vitro*, and for the first time we investigate the role of CPE in orthotopic GBM mouse models.

3. MATERIALS AND METHODS

3.1 MATERIALS

3.1.1 MACHINES

Machine	Model	Producer
Incubators	CO_2-Incubator	Sanyo; Munich, Germany
Microscopes and Cameras	Eclipse TS100	Nikon; Kingston, England
Neugebauer counting chambers		Marienfeld; Bad Mergentheim, Germany
Shaker		
Sterile-Bench	Hera Safe	Heraeus; Hanau, Germany
Vortexer	MS1 minishaker	IKA Works; Wilmington USA
Heating block	Grant QBT4	Grant; Cambridge, England
ELISA-Reader	Thermo Electron Multiscan EX	Thermo Electron Corporation; Karlsruhe, Germany
Gel documentation device	ChemiDoc™ Imaging System	Biorad; Munich, Germany

Multipette		Eppendorf; Hamburg, Germany
Spectrophotometer	NanoDrop ND 1000	Peqlab; Erlangen, Germany
Power source	Power Pac	Biorad; Munich, Germany
centrifuge	Multifuge 3 S-R	Heraeus; Hanau, Germany
Table centrifuge	Biofuge Pico	Heraeus; Hanau, Germany
Immunoblot Apparatus	Biorad	Biorad; Munich, Germany
Stereotactic apparatus	Stoelting	Stoelting, Dublin, Ireland
automatic injection device	Leica nanoinjector stepper motor precision	Leica microsysteme, Wetzlar, Germany
Irradiator	^{137}Cs Gammacell GC40	Best Theratronics, Ontario, Canada
Thermal cycler	Applied Biosystems 7500 Fast Real-Time PCR System	Thermo Fisher Scientific, Darmstadt, Germany

3.1.2 MATERIALS

Materials	Producer
Filter tips 0.1 – 10 / 10 – 100 / 20 – 200 / 100 – 1000 µl	Gilson; Middelton, USA
plastic pasteur pipetts	Ratiolab; Dreieich, Germany
Pasteur pipetts	WU; Mainz Germany
Plastic pipetts 5 / 10 / 25 / 50 ml	Corning; New York, USA
Pipett tips 0.1 – 10 / 10 – 100 / 20 – 200 / 100 – 1000 µl	Ratiolab; Dreieich, Germany
Glass slides 26 x 76 mm	Langenbrinck; Emmendingen, Germany
Falcon 15 / 50 ml	Corning; New York, USA
Reaction tubes with lid 1,5 / 2 ml	Greiner Bio-One; Frickenhausen, Germany
Hypodermic needles	Braun; Meisungen, Germany
Cell culture flasks	Greiner Bio-One; Frickenhausen, Germany
Cell culture plates	Corning; New York, USA
parafilm	Pechiney; Chicago, USA
PVDF membrane	Carl Roth; Karlsruhe, Germany
Cell culture inserts	Schubert & Weiss OMNILAB, Munich, Germany
Hamilton syringe10µl	MedChrom, Dalsheim, Germany
Perma-hand seide (suture material)	Ethicon, Livingstone, Scotlaand

Sterile surgical blades	Braun Aesculap, Tuttlingen, Germany
Optical adhesive film	Thermo Fisher Scientific, Darmstadt, Germany
ABGene PCR plates	Thermo Fisher Scientific, Darmstadt, Germany

3.1.3 CHEMICALS

Chemical	Producer
Ammonium persulfate (APS)	Carl Roth; Karlsruhe, Germany
Bovines Serum Albumin (BSA)	Carl Roth; Karlsruhe, Germany
Calcium chloride ($CaCl_2$)	Sigma-Aldrich; Steinheim, Germany
Dimethyl sulfoxide (DMSO)	Carl Roth; Karlsruhe, Germany
Dithiothreitol (DTT)	Carl Roth; Karlsruhe, Germany
Ethanol 99%	Merck; Darmstadt, Germany
Glycerol	Carl Roth; Karlsruhe, Germany
Glycin	Carl Roth; Karlsruhe, Germany
Skim milk powder	Carl Roth; Karlsruhe, Germany
Methanol	VWR; Darmstadt, Germany
Hydrochloric acid (HCl) (37%)	Carl Roth; Karlsruhe, Germany
Sodium dodecyl sulphate	Carl Roth; Karlsruhe,

(SDS)	Germany
Tetramethylethylediamine (TEMED)	Carl Roth; Karlsruhe, Germany
Tris Base	Sigma-Aldrich; Steinheim, Germany
Triton X-100	Sigma-Aldrich; Steinheim, Germany
Acrylamide	Carl Roth; Karlsruhe, Germany
Bradford Reagent	Carl Roth; Karlsruhe, Germany
Bromophenol blue	Merck; Darmstadt, Germany
Isopropanol	Merck; Darmstadt, Germany
Igepal (NP-40)	Sigma-Aldrich; Steinheim, Germany
Sodium chloride	Merck; Darmstadt, Germany
Tween-20	Carl Roth; Karlsruhe, Germany
Potassium chloride	Carl Roth; Karlsruhe, Germany
Magnesium chloride	Carl Roth; Karlsruhe, Germany
Hydroxyethylpiperazine ethane sulfonic acid (HEPES)	Carl Roth; Karlsruhe, Germany
Ethylenediaminetetraacetic acid (EDTA)	Sigma-Aldrich; Steinheim, Germany
Sodium azide (NaN_3)	Carl Roth; Karlsruhe, Germany
Acetic acid	Carl Roth; Karlsruhe, Germany
Diethyl pyrocarbonate (DEPC)	Sigma-Aldrich; Steinheim, Germany

3.1.4 OTHER SUBSTANCES

Substance	Producer
Full Range Rainbow Molecular Weight Marker	PanReac AppliChem; Darmstadt, Germany
Proteinase K (20mg/mL)	G Bioscience; St. Louis, USA
Phospho-Stop	Roche; Mannheim, Germany
WesternBright ECL HRP Substrate	Advansta; California, USA
Mayer's Hematoxylin solution	Merck, Darmstadt, Germany
Moviol	Carl Roth; Karlsruhe, Germany
Decosept AF	Dr Schuhmacher; Malsfeld-Beisefórth, Germany
Carpofen, Antidots, Narcotics	Veterinary Support Unit, University of Tuebingen
Bepanthen	Bayer Vital, Leverkusen, Germany
PeqGOLD TriFAST (Trizol)	PeqLAB, Germany
Oligo-d(T_{20})	Sigma-Aldrich; Steinheim, Germany
M-MLV Reverse Transcriptase	Promega, Mannheim, Germany
Viromer BLUE	Biozym, Hessisch Oldendorf, Germany
dNTP mix	PeqLAB, Germany

3.1.5 KITS

Kit	Producer
NucleoSpin RNA plus	Machery-Nagel, Dueren, Germany
MycoAlert Mycoplasma Detection Kit	Lonza; Köln, Germany
SensiMix SYBR low-Rox KIT	Bioline, Berlin, Germany
Pierce BCA Protein assay kit	Thermo Fisher Scientific, Darmstadt, Germany

3.1.6 CELL CULTURE

Medium / Supplement	Producer
Puromycin	Applichem, Darmstadt, Germany
Dulbecco's modified eagle medium (DMEM)	Sigma-Aldrich; Steinheim, Germany
Fetal Bovine Serum (FBS)	Sigma-Aldrich; Steinheim, Germany
G418 sulfate	Biochrom, Berlin, Germany
PBS-DULBECCO	Sigma-Aldrich; Steinheim, Germany
Recombinant human „Epidermal Growth Factor" (EGF)	Biomol; Hamburg, Germany
Trypsin	Sigma-Aldrich; Steinheim, Germany

Acutase	Sigma-Aldrich; Steinheim, Germany
Mitomycin C	Sigma-Aldrich; Steinheim, Germany
Penicillin/Streptomycin	PAA Laboratories; Cölbe, Germany
U-0126 MEK inhibitor	Selleckchem, Munich, Germany
S3I-201 STAT3 inhibitor	Sigma-Aldrich; Steinheim, Germany
Temozolomide (TMZ)	Sigma-Aldrich; Steinheim, Germany
Lentivirus LPP-NEG-Lv105-025-C	GeneCopoeia, Rockville, Maryland
Lentivirus LPP-FO192-Lv-105-050-S (expressing human CPE)	GeneCopoeia, Rockville, Maryland
MISSON esiRNA human SNAI2	Sigma-Aldrich; Steinheim, Germany
MISSION esiRNA Egfp	Sigma-Aldrich; Steinheim, Germany
Ad-CMV-EGFP	Vector Biolabs, USA

3.1.7 SOFTWARES

Software	**Producer**
Word Office	Microsoft
Power Point Office	Microsoft
Excel Office	Microsoft
ImageJ	Fiji
Image Lab Version 5.1	Biorad
Ascent Software 2.6	Thermo Fisher Scientific
Inveon Research Workplace 3.1	Siemens Preclinical Solutions

3.2 METHODS

3.2.1 Cell lines and cell culture

LNT-229 and LN-308 cells were kindly provided by N. de Tribolet (Lausanne, Switzerland) and T98G cells were provided by American Type Culture Collection (ATCC, Wesel, Germany). These cell lines were characterized for main mutations involved in cancer progression by Ishii et al. and their genotype is reported in Table 3.2.1. GBM primary cells Tu-132 and Tu-140 were generated from human grade II glioma (71 year old male patient) and human grade IV GBM (41 years old female) specimens respectively and used at passage 3-10. All cells were maintained in DMEM, containing 10% FBS, penicillin (100 U/ml)/streptomycin (100 μg/ml) and the appropriate selection antibiotics in a humidified atmosphere containing 5% CO_2 at 37°C. Cells were splitted at approximately 80% confluency. The cells were routinely treated with BioMyc1 and BioMyc2 and tested for mycoplasma contamination prior to the experiments. Only mycoplasma-negative cells were used for experiments.

Rat CPE-overexpressing cells were generated by transfection with pcDNA3-CPE (LNT-229-rCPE) or the

empty control vector pcDNA3 (LNT-229-neo) as previousely described [51]. At least 2 different cell clones were used in the analyses.

Table 3.2.1Cell lines characterization [82]

CELL LINE	p53	PTEN	$p16^{INK4A}$	$p14^{ARF}$
LNT-229	(i) Heterozygotic wildtype – mutant CCT(Pro)→CTT(Lys) (ii) 100% transcriptional activity based on reporter genes analyses	wildtype	deleted	deleted
LN-308	deleted	splice (deletion exon 6)	wildtype	wildtype
T98G	mutated ATG(Met)→ATA(Ile)	mutated CTT(Leu)→ CGT(Arg)	deleted	deleted

3.2.2 Generation of human CPE-overexpressing cells

Stable human CPE-overexpressing glioma cells were generated by lentiviral transduction. The cells were seeded in 24-well plates ($4x10^4$cells/well/500µl) in complete growth medium and allowed to attach overnight. For each well, 500 µl of virus suspension was prepared in complete growth medium containing 5µg/ml polybrene and 10 MOI (Multiplicity of infection) of pReceiver-LV105 lentivirus expressing human CPE and control of the CMV promoter

and the selection marker gene for puromycin resistance, or its empty counterpart. Culture medium was removed and replaced with 500 µl of viral supernatant. Plates were placed for 2 hours at 4°C and were afterwards transferred to 37°C. The next day the virus containing medium was replaced by fresh growth medium. 72 hours after transduction the cells were transferred to 6-well plates and selection was started by adding puromycin (2 µg/ml). CPE overexpression and secretion was analyzed by immunoblot every 5^{th} passage.

3.2.3 Experimental treatment

For the experiments, cells were seeded in complete growth medium in 6-, 12-, 24- or 96- well plates depending on the experiment and allowed to attach. After 24 hours, culture medium was substituted by growth medium or serum free medium (SFM) supplemented with the agents indicated for each experiment. U0126, a specific MEK inhibitor, was used at the concentration of 10 µM and S3I-20, a STAT3 inhibitor, at the concentration of 30 µM. Temozolomide (TMZ) was used at different concentration ranging from 0.3 to 3 µM. For irradiation, cells were irradiated with 2 or 4 Gy in a ^{137}Cs Gammacell GC40.EGF (10µM) treated

cells were used to generate positive controls for either phosphor-ERK1/2 or phospho-STAT3.

3.2.4 Transcriptome and miRNAome profiling experiments

Sample preparation

LNT-229-neo and –rCPE cells were used in these analyses in triplicates. Cell pellets from $1.5x10^7$ cells were generated and were resolved in 1.5 ml of Trizol, homogenized by inversion and incubated at room temperature for 5 minutes. After centrifugation, 300 µl of chloroform were added to the pellet and vortexed for 15 seconds. Samples were left 10min at room temperature and then centrifuged at 12,000 rpm for 15 minutes at 4°C. The aqueous phase was transferred into a new tube. 750ul of isopropanol were added for precipitation. After incubation for 10 minutes at room temperature, samples were centrifuged at 12,000 rpm for 30 minutes at 4°C. Pellets were rinsed twice with EtOH 75%, dried, resuspended in 200 µl of DEPC-treated RNase-free water and stored at -80°C. Samples were sent in dry ice for further analysis to the Genomics and Proteomics Research Unit, Department of Oncology, Luxembourg Institute of Health (L.I.H.) Luxembourg.

Analysis

Analysis was performed and method description was provided by T. Kaoma (Genomics and Proteomics Research Unit, Department of Oncology, Luxembourg Institute of Health (L.I.H.) Luxembourg). RNA purity and integrity were monitored using NanoDrop® ND-1000 spectrophotometer and Agilent 2100 Bioanalyzer with RNA 6000 Nano assay kit. Only RNAs with no sign of contamination or marked degradation (RNA integrity number (RIN) > 9) were considered good quality and used for further analysis. Transcriptome and miRNAome profiles were determined in triplicate RNA samples using the Affymetrix Human Transcriptome Array (HTA) 2.0 and miRNA 4.0 Genechip arrays, respectively. For whole-transcript expression analysis, 100 ng of total RNA was processed and labeled using the GeneChip WT PLUS Reagent kit (Affymetrix), whereas for miRNA analysis, 500 ng of total RNA was processed using the FlashTag Biotin HSR RNA labelling kit (Genisphere, USA) according to the manufacturer's standard protocols (P/N 4425209 Rev.B 05/2009, P/N 702808 Rev.6, and P/N 703095 Rev3). Upon hybridization of labeled products, arrays were washed and stained using the Affymetrix

GeneChip WT Terminal Labeling and Hybridization kit, before being scanned using a GeneChip Scanner 3000.

3.2.5 Microarray data analysis

Analysis was performed in collaboration with A. Mueller (NORLUX Neuro-Oncology Laboratory, Luxembourg Institute of Health, Luxembourg) who also provided the methods description. CEL files generated upon array scanning were imported into Partek® Genomics Suite TM (GS) 6.6 for preprocessing. Partek was set up to run standard Robust Multi-array Average (RMA) at the probeset level. Resulting log2 probeset intensities were then imported into R statistical environment (http://www.R-project.org/) for further analysis. First, log2 intensity values were summarized to estimate the expression level of each transcript cluster (TC) by averaging the intensity signals from the corresponding probeset regions. Matching between probesets, TCs and targeted genes was verified through Affymetrix annotation files (HTA-2_0 probeset and transcript hg19 na33.1 csv file). The quality of the data was then evaluated by assessing repeatability Pearson's correlation coefficients, and through visual inspection of density plots and relative-log expression plots. Principal component analysis was also

used to reduce dimensionality of the data, visualize the concordance between biological replicates, and assess if the variability in data actually reflected what was expected from the experimental design. Finally, the LIMMA package (R/Bioconductor) was used to estimate the statistical significance of TC expression level differences between LNT-229-rCPE and LNT-229-neo samples as the reference. Resulting p-values were adjusted for multiple testing error using the Benjamini and Hochberg' false discovery rate (FDR) [83]. Elements with a FDR less than 0.05 were considered as differentially expressed (DE), irrespective of the fold-change.

MiR chip data were analyzed similarly as HTA data with some adjustments. First, intensity signals from probesets targeting non-human transcripts were filtered out from the analysis. Second, no summarization of intensity signals was performed as the design of miRNA 4.0 did not include any TC level. Microarray expression data are available at ArrayExpress (http://www.ebi.ac.uk/arrayexpress/) under the accession numbers E-MTAB-5297 and 5299. Transcript clusters with FDR < 0.05 were considered as significantly differentially expressed. The QIAGEN's Ingenuity® Pathway Analysis software (IPA®, QIAGEN Redwood City, www.qiagen.com/ingenuity) was used for

transcript cluster mapping and data mining including functional analyses, upstream analysis and gene network reconstruction. Right-tailed Fisher's exact test was used to calculate a p-value for functional enrichment analysis (threshold: -log(p-value) > 1.301). Identification of differentially regulated miRNAs associated with the regulation of cell motility was reached by a combined analysis of IPA and open access softwares: mirtargetlink (https://ccb-web.cs.uni-saarland.de/mirtargetlink), RefGene (www.refgene.com), mirtarbase (www.mirtarbase.mbc.nctu.edu). IPA analyses was based on significant mRNA (FDR<0.01) and miRNA (FDR<0.05) and on the following criteria: (i) there is a known miRNA - mRNA target interaction described and (ii) the expression pairing must be opposite (either mRNA downregulated and miRNA upregulated or vice versa).

3.2.6 RNA preparation and quantitative RT-PCR

For RNA preparation $5x10^5$ cells were seeded in growth medium in 6-well plates, were allowed to attach overnight and subsequent medium change. At defined time points (mainly 24h or otherwise as specified) the cells were washed once, scraped and re-suspended in cold PBS. Cells were harvested by centrifugation (1200 rpm, 5 min.). Total

RNA was isolated from cell pellets using NucleoSpin RNA plus columns. RNA purity and concentration was measured using Nanodrop. 5 µg of RNA, mixed with oligo-dT_{20} (10ng/µl) and dNTPs (0,5 mM), was reverse-transcripted using M-MLV Reverse Transcriptase (200 U) in a total volume of 20 µl. 5 µl of 1:10 diluted cDNA of each sample was used in a total volume of 15 µl of 2x PCR mix (SensiMix SYBR low-Rox KIT), along with gene specific forward and reverse primers (250 nM) as listed in Table 3.2.2. PCR protocol includes 40 cycles of: 95 °C (30 s), 56 °C (30 s) and 72 °C (30 s). A reference sample (RS) was included in every RT-PCR to allow comparison of different RT-PCR runs. Relative mRNA expression of each gene of interest (GOI) was quantified by using PRPL0 or GAPDH as housekeeping control genes.

$\Delta CT = CT(GOI) - CT(housekeeping)$

$\Delta\Delta CT = \Delta CT(sample) - \Delta CT(RS)$

n-fold expression= $2^{\Delta\Delta CT(GOI)}$

Table 3.2.2 Primers list

GENE	FORWARD	REVERSE
MGST1	GGTTTTGTTTATGGTAC TTCAGAGT	TGTGAATTGTTCATTTA GATGTGCC
PCDH17	AGTTTGTTCAAAGTAGC TCCACG	TCACAGCAGGAGCCTTT GTT
PTPRD	ATGTCAGAGAGCTGCG AGAA	TAAGGCATTGGTGACCC CAC
MGAT4A	TGGTGTTGCAGAAGGA ATGGT	TCAGATGATCAGTTGGT GGCT
SNAI2	CATACCACAACCAGAG ATCC	GAGGAGTATCCGGAAA GAGG
ADAMST 4	GACAAGTGCATGGTGT GCG	GCCGGACAAGAATGTG GGT
CD9	AAACGCTGAAAGCCAT CCAC	GATGGCATCAGGACAG GACTT
CDCA7L	TTTAACGCCCCCAGTGA TGA	GACTCCACGACCTGTTT CCC
SPP1	GCCGAGGTGATAGTGT GGTT	ACGGCTGTCCCAATCAG AAG
CDKN1A (P21)	GATGACAAGCAGAGAG CCCC	ACTCCCCACATAGCCCG TAT
STC1	AAGATGGCGACCACCA AAGT	GCAGTGACGCTCATAA GGGA
PRPL0	GAGTCCTGGCCTTGTCT GTGG	TCCGACTCTTCCTTGGC TTCA
GAPDH	TCAACGGATTTGGTCGT ATTGG	CTTCCCGTTCTCAGCCT TGAC
rCPE	ATGGCCGGGCGCGGAG GAC	CAGCTCGATGACCAGG AGCTC
huCPE	ATGGGAATGAGGCTGT TGGAC	GGCATGATGTGAATGC GGGTA

3.2.7 Western blot

For cell lysates $5x10^5$ cells were treated as indicated, washed once with ice-cold PBS, scraped, re-suspended in cold PBS and centrifuged (5 min, 1200 rpm). Cell pellets were lysed in lysis buffer (Table 3.2.3) for 15 minutes on ice, centrifuged 15 minutes at 13.000g to remove the not soluble fraction, and clarified cell extracts were transferred to new vials. Protein determination was performed using the Bradford assay [84]. Cell pellets collected for EGFR detection were lysed in RIPA buffer (Table 3.2.3) and protein concentration was determined using the BCA assay [85].

For the preparation of secreted proteins, $5x10^5$ cells were treated under serum free conditions and supernatants were collected 48 h later. Cell debris were removed by centrifugation and protein concentration was analyzed as described before. 30 μg of secreted protein (otherwise specified) were precipitated using 3 volumes of ice-cold acetone and dried. Proteins were re-suspended in Laemmli buffer (Table 3.2.3), heated at 95 °C for 10 min and loaded on 8% or 10% gels for SDS-PAGE (Table 3.2.3). Electrophoresis was performed at 200 mV in running buffer (Table 3.2.3). Transfer on PVFD membranes using transfer buffer (Table 3.2.3) was performed at 100 mV for

1 hour or 25mV overnight for EGFR detection. Membranes were blocked in blocking buffer (Table 3.2.3) for 1 h, exposed overnight to the primary antibody (Table 3.2.4) in TS-TMBSA (Table 3.2.3) at 4 °C. After washing, blots were exposed for 1 h to HRP-conjugated anti-mouse or anti-rabbit secondary antibody (1:10.000, Table 3.2.4) Immunoreactivity was visualized with Chemiluminescent HRP Substrate and detected with ChemiDoc™ Imaging System. GAPDH or Tubulin was used as loading controls. Poinceau S staining was performed to prove correct loading of secreted proteins.

Table 3.2.3 Western blot buffers

solution	
Lysis buffer	50 mM Tris-HCl, pH=8, 120 mM NaCl, 5mM EDTA, 0.5% NP-40, phosphatase inhibitor, protease inhibitor
RIPA buffer	50 mM Tris-HCl, pH=8, 150 mM NaCl, 1% NP-40, deoxycholate 0.5 %, SDS 0.1 %, phosphatase inhibitor, protease inhibitor
Laemmli buffer	100 mM Tris HCl pH 6.8, 4% SDS, 0.2% bromphenol blue, 20 % glycerol, 10% 2-mercaptoethanol
Resolving gel	30% acrylamide mix, 1.5 M Tris-HCl, pH=8.8, 8-10% SDS, 10% APS, TEMED, dd H_2O
Stacking gel	30% acrylamide mix , 0.5 M Tris-HCl, pH=6.8, 10% SDS, 10% APS, TEMED, dd H_2O
Running buffer	5 mM Tris HCl, 38.6 mM Glycine
Transfer buffer	2.5 mM Tris HCl, 19.2 mM Glycine, 20 % methanol
TBS	50 mM Tris HCl, 150 mM NaCl, 0.05% v/v Tween-20
TS-TMBSA	10 mM Tris HCl, 150 mM NaCl, 0.1 % Tween 20, 5 % skim milk powder, 2 % BSA, 0.001 % sodium azide, pH was set to 7.4

Table 3.2.4 Antibody list

antibody	Ref. number	Provider
Slug (C19G7) Rabbit mAb	#9585	Cell signaling
p21 Waf1/Cip1 (12D1) Rabbit mAb	#2947	Cell signaling
Anti-α tubulin (rabbit)	sc-12462-R	Santa Cruz Biotechnology
Mouse polyclonal anti-human TIMP-2	Mab971	R&D Systems; Minneapolis, USA
Rabbit monoclonal anti-human MMP-14	2010-1	Epitomics; Burlingame CA, USA
Rabbit anti-human MMP-2	#4022	Cell signaling
Anti-GAPDH (rabbit)	sc-25778	Santa Cruz Biotechnology
Purified mouse anti-Carboxypeptidase E	NBP2-15699	Novus
Anti-Bcl2 (mouse)	sc-509	Santa Cruz Biotechnology
Stat3 (124H6) Mouse mAb	#9139	Cells signaling
Phospho-Stat3 (Ser727) Antibody (rabbit)	#9134	Cell signaling
Anti-ERK1/2 (mouse)	sc-135900	Santa Cruz Biotechnology
PathScan® Multiplex Western Cocktail I: Phospho-p90RSK, Phospho-Akt, Phospho-p44/42 MAPK (Erk1/2) and Phospho-S6 Ribosomal Protein Detection Cocktail I	#5301	Cell signaling

Phospho- EGFR Receptor Antibody Sampler Kit	#9922	Cell signaling
Goat anti-mouse IgG-HRP	sc-2005	Santa Cruz Biotechnology
Goat anti-rabbit IgG-HRP	sc-2004	Santa Cruz Biotechnology

3.2.8 Proliferation assay

Cells were seeded in growth medium in 96-well plates ($1x10^4$ or $5x10^4$) and allowed to attach overnight before treatment. Cell growth was analyzed using crystal violet staining as described [86]. Stained cells were solved in natrium citrate and absorbance was measured at 570 nm as indication of cell density.

3.2.9 Migration measurements

Migration was measured using either wound healing (scratch) assay or transwell migration chambers. For the wound healing scratch assay $3x10^5$ cells were seeded in growth medium in 12-well plate and allowed to attach. The scratch was performed using a 100 or 1000 µl pipette tip and debris was removed by washing the cells. Migration was monitored photographically at defined time points.

In transwell migration assays $2x10^4$ cells were seeded in the upper layer of 8 µm pore-sized Boyden transwell chambers. Cells were allowed to actively migrate for 18

hours towards FCS containing DMEM as attractant medium placed in the bottom chamber. Cell from the upper part of the membrane were removed using Q-tips. Migrated cells on the lower layer of the membrane were fixed in cold methanol for 10 min., stained with Mayer's Hematoxylin solution for 20 minutes and washed in water. The membranes were transferred to glass slides and covered using Moviol. Stained cells were counted and seven areas for each membrane were taken for analysis. Number of migrated cells was normalized to the total number of cell, assessed in parallel as cell density by cristal violet staining.

3.2.10 Clonogenic survival assay

250 cells were seeded in growth medium in 6-well plates, allowed to attach and irradiated (0, 2 or 4 Gy). Alternatively, the cells were treated with TMZ (0, 3 ,1 or 3 μM) for 24 h. After treatment, the medium was replaced and after 2 weeks cell colonies were stained using crystal violet. Visible colonies (> 50 cells) were counted and the survival fraction was calculated according to the following formula:

plating efficiency(PE) = number of colonies counted/number of cells plated *100

survival fraction(SF) = PE of treated sample/PE of control *100

The Webb method was used to calculate synergism [87].

3.2.11 Infection of cells with recombinant adenovirus

3,5 x 10^5 cells were seeded in growth medium, allowed to attach and were infected with Ad-CMV-SNAI2 or Ad-CMV-EGFP as negative control. The construction of Ad-EGFP has been described [88]. For the generation of Ad-SLUG, human SNAI2/SLUG cDNA was cloned into pTRACK-CMV using the Ad-Easy system provided by B. Vogelstein (Baltimore, MD, USA) [89].

3.2.12 Transfection of cells with si-RNA

8 x 10^4 cells were seeded in 24-well plates in and allowed to attach. Transfection was performed using the ViromerBlue transfection kit. siRNA constructs (siSNAI2 or siEGFP as negative control) were diluted in Buffer Blue at the concentraction of 2.8 µM, mixed with a 1:9 solution of Viromer Blue and Buffer Blue and let 15 min RT. 50 µl were added in complete growth medium in each well at the final concentration of 25 mM. After 24 hours, cells were lysed for RNA collection or seeded for cell transwell migration. Detailed protocols can be found at https://viromer-transfection.com.

3.2.13 Animal experiment

4-weeks-old female mice athymic FoxN1-deficient NMRI nude mice were purchased from Janvier (St. Berthevin, France). Mice were kept in filter-top cages at 22 °C, 60% humidity. Sterilized food and water were accessible ad libidum. Animals were anesthetized by intraperitoneal injection (0,1 ml/10g) of a mixture of 3-components-narcotic (0,5 mg/kg Medetomidin, 5 mg/kg Midazolam and 0,05 mg/kg Fentanyl). LNT-229-neo or -rCPE cells (2 independent experiments), LNT-229-ctrl or –hu-CPE cells or LN-308-ctrl or -huCPE were used in the animal experiments. 10^5 cells were injected intracranially in 2 µl PBS in the right striatum. Anesthesia was abrogated by subcutaneous injection (0,1 ml/10g) of antidot mixture (1,2 mg/kg Naloxon, 0,5 mg/kg Flumazenil and 2.5 mg/kg Atipamezol). For analgesis, 0,1 ml/10g of Carprofen was injected subcutaneously. Mice were weighted and checked three times a week and were sacrified at appearance of neurological symptoms. Survival was evaluated by performing Kaplan-Meier survival analyses.

3.2.14 MRI imaging

MRI imaging of mice was performed in collaboration with M. Krüger (Werner Siemens Imaging Center, Department

of Preclinical Imaging and Radiopharmacy, Eberhard Karls University, Tuebingen, Germany). On different days post implantation of tumor cells, animals were anesthetized with a mixture of 1.5% isoflurane (Abbott, Wiesbaden, Germany) evaporated in oxygen at a flow of 0.5 l/min. Subsequently, animals were placed in a 1 T Icon-Scanner (Bruker, Ettlingen, Germany) equipped with a mouse brain coil and T2-weighted images of the brain were acquired. Body temperature was maintained at 37 °C by a heating system and a rectal temperature sensor. Tumor volumes were determined by manually drawing regions of interest in the MR images in Inveon Research Workplace 3.1 (Siemens Preclinical Solutions, Erlangen, Germany) and creating volumes of interest

3.2.15 Statistic analysis

The figures show data obtained in at least three independent experiments as indicated. Statistical analyses were performed using Excel, Microsoft. Quantitative data was assessed for significance by t test (*$p < 0.05$; **$p < 0.01$; ***$p < 0.005$). Statistical analysis for clonogenic survival assay was performed used the Webb Method [87]. Survival of mice was analyzed by Kaplan-Meier life tables.

Wilcoxon and log-rank test were used for comparison of survival (significance level $\alpha = 0.05$).

4. RESULTS

4.1 Effects of CPE on proliferation and migration of GBM cells

In a recent publication of our lab it has been shown that overexpression of rat CPE on the one hand mitigates migration of glioma cells and on the other hand induces proliferation [51], indicating that CPE might be a switch factor regulating the "Grow or Go" behavior of glioma cells.

For this we generated, besides rat CPE-overexpressing LNT-229 cells that are available in the lab, human CPE-overexpressing glioma cell lines using lentiviral transdution. Expression of sCPE was demonstrated in cell supernatants generated from LNT-229-rCPE and lentivirally huCPE transduced LNT-229, T98G, LN-308 and Tu-132 glioma cells and their control transduced counterparts (Figure 4.1.1).

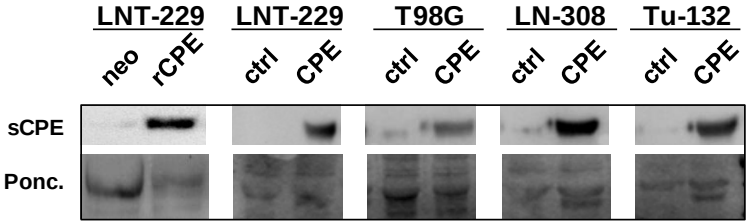

Figure 4.1.1 Analysis of sCPE secretion in CPE-overexpressing GBM cells. Immunoblot detection of sCPE in supernatants derived from CPE-overexpressing LNT-229 (either rat or human CPE), T98G, LN-308 and Tu-132 cells. Ponceau staining was used to demonstrate equal protein loading (n = 3, one representative experiment is shown).

In colorectal cancer (CRC) it has been shown that CPE modulates proliferation through modulation of cell cycle regulator p21 [79]. Therefore we analyzed p21 expression in CPE-overexpressing GBM cells (Figure 4.1.2) and found lower levels of p21 in all CPE-overexpressing cells.

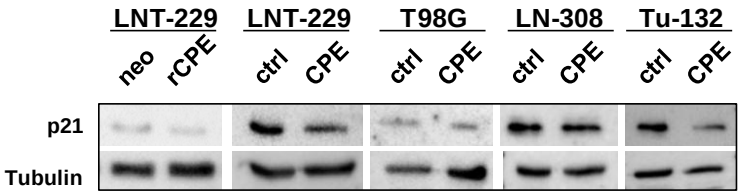

Figure 4.1.2 CPE modulates p21 expression in GBM cells. Immunoblot detection of p21 in CPE-overexpressing LNT-229 (either rat or human CPE), T98G, LN-308 and Tu-132 cells. Tubulin was used as a loading control. (n = 3, one representative experiment is shown)

Nevertheless, significant differences in cell density overtime, indicating enhanced proliferation, were observed only in rCPE-overexpressing LNT-229 clonal cell lines as already shown by Höring et al [51]. No significant differences were observed in human CPE-overexpressing cells, except for a few time points: day 4 for T98G cell line and day 6 for LNT-229 (Figure 4.1.3).

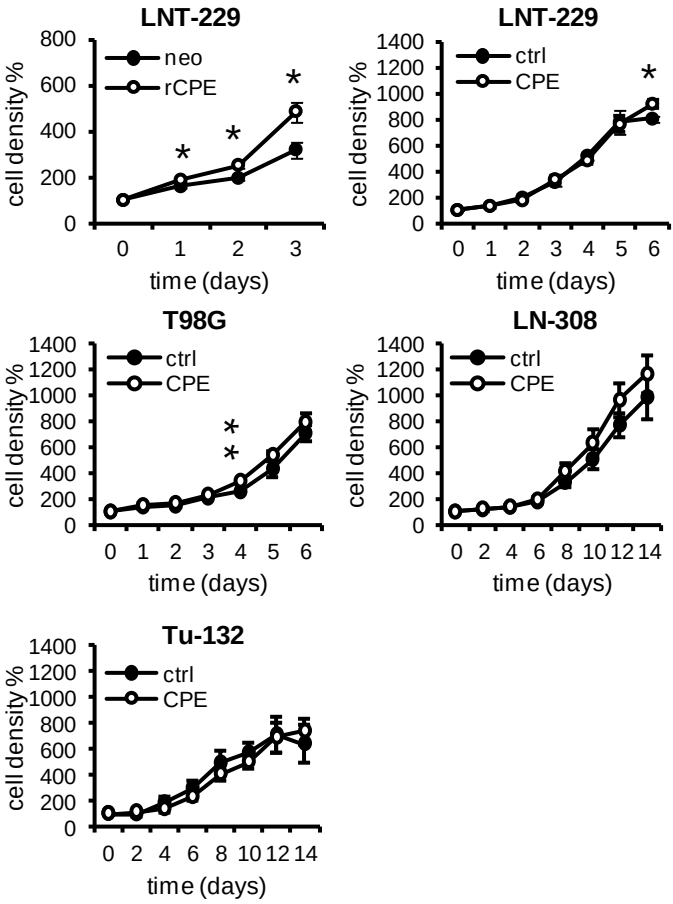

Figure 4.1.3 Effects of CPE overexpression on the proliferation of GBM cells. Cell growth was analyzed in CPE-overexpressing LNT-229 (either rat or human), T98G, LN-308 and Tu-132 or their sibling control cells. Crystal violet staining performed every 24 hours for LNT-229 (n=6) and T98G (n=3), every 48 hours for LN-308 (n=6) and Tu-132 (n=3, SEM, * $p < 0.05$, ** $p < 0.01$).

Using transwell migration chambers (Figure 4.1.4) we showed that overexpression of CPE led to a significant reduction in the number of migrated cells in all GBM cell lines and primary GBM cells tested so far. The same effect of CPE was previously described by Höring et al for rCPE-overexpressing clonal LNT-229 and LN-308 glioma cell lines [51]. Consistently and as demonstrated before for LNT-229 cells [51], siRNA-mediated downregulation of CPE in highly CPE-expressing Tu-140 glioma primary cells induces cell motility (experiment performed by our collaborator E. Ilina, Goethe University, Frankfurt). These data prompted us to focus on the effects of CPE on glioma cell motility, considering that CPE effects on cell growth may be species-specific, whilst a general effect of both rat and human CPE on migration has been demonstrated.

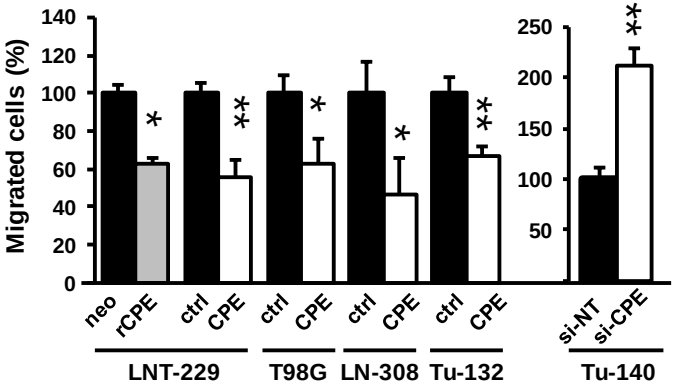

Figure 4.1.4 Effects of CPE on the migration of GBM cells. Cell migration was analyzed by using transwell migration chambers. Right panel: migration of LNT-229, T98G, LN-308 and Tu-132 control (black bars), rat CPE- (gray bars) or human CPE- (white bars) overexpressing cells (n=3, SEM); left panel: migration of Tu-140 cells 48 h after transfection with either siCPE or non-target siRNA (si-NT; n=3, SEM). The latter experiment was performed by E. Ilina, Goethe University, Frankfurt. * $p < 0,05$, **$p<0,01$.

4.2 Transcriptome analyses: CPE modulates mRNA as well miRNA expression associated to signal transduction cascades and genes involved in the regulation of cell motility

As demonstrated in chapter 4.1, sCPE significantly mitigates glioma cell migration. Since sCPE is, at least partially, responsible of this effect, the extracellular signal provided by sCPE has to be transmitted to the intracellular compartment to provide the anti-migratory function of sCPE. We hypothesize that the sCPE-mediated reduction of glioma cell migration will be associated with changes in the expression of motiliy-associated genes. We therefore performed mRNA and miRNA expression micro-array analyses of faster migrating LNT-229-neo and slower migrating LNT-229-rCPE cells. Using mRNA expression microarray and IPA, we found with a false discovery rate (FDR) of < 0.01 that 1065 mRNA were differentially expressed. In this cohort, at least 100 genes were either directly or indirectly connected to the regulation of cell motility (Supplementary Table 1).

In LNT-229-rCPE cells we found by IPA an enrichment of differentially expressed mRNAs that are associated to the CDC42-, FAK-, STAT3-, TGF-β-, PAK- and integrin-

signaling pathways, all known to regulate migration and all known to be involved in carcinogenesis or tumor progression (Figure 4.2.1, Table 4.2.1). Even though the Z-score, an indicator of pathway activation/inactivation, did not reach significance, there is a tendency detectable that the CDC42-, TGF-β-, PAK- and integrin signalling cascades are less activated in LNT-229-rCPE cells. Missing significance in this analysis could be explained by the algorithm of the IPA software since this program does not take into consideration the literature available for glioma due to the high similarity of available gliomas gene profiles and of our glioma samples.

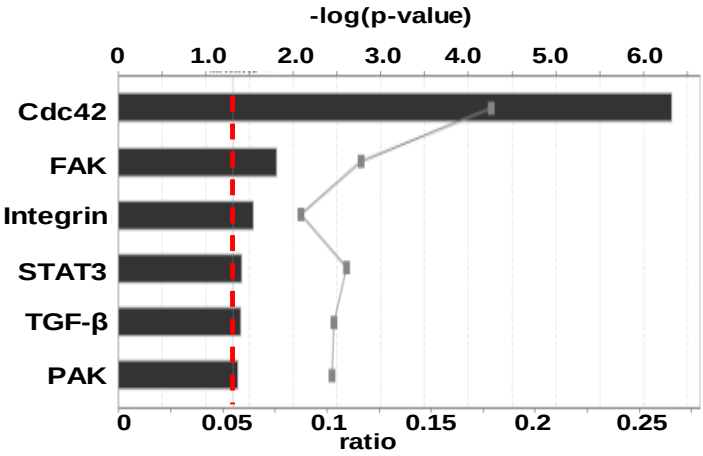

Figure 4.2.1 Canonical pathway analyses. IPA based analysis of differential gene expression in LNT-229-rCPE versus -neo cells and their association to signaling networks representing enriched (pValue < 0.05) canonical pathway considered as important in cell motility.

To confirm microarray derived changes in the expression of motility-associated genes, we exemplarily validated CPE-induces changes in the expression of assorted genes using quantitative reverse-transcription PCR (qRT-PCR). Since cell motility is a complex process involving cell adhesion, destruction of the cellular matrix, modification of the cell architecture and others, we evaluated genes involved in different processes influencing cell motility (Figure 4.2.2). In LNT-229-rCPE *osteopontin* (OPN/SPP1),

a secreted, pro-migratory factor, was downregulated (10.1 x down). *Stanniocalcin-1* (STC1), a marker-gene for glioma progression and known to be a hypoxia-dependent migration factor in glioma, was also downregulated (1.6 x down) while *procaherin-17* (PCDH17) which regulates actin dynamics and is known to inhibit metastasis and invasion of HCC cells, was upregulated (4.7 x up). *Tetraspanin* (CD9), known to inhibit CD26-mediated invasion of mesenthelioma, was upregulated (3.5 x up). qRT-PCR confirm the micro-array data in regard to the expression of enzymes involved in the destruction and modulation of the extracellular matrix. Additionally, *a disintegrin and metalloprotease with thrombospondin motifs* (ADAMTS4, 3.3 x down), N-Acetyl-Glucosamyl-Transferase IV A (MGAT4A, 3.2 x down) the stem cell marker *SRY-box 2* (SOX2, 2.6 x down) as well as the pro-migratory *SNAIL-family zink finger 2 protein* (SNAI2/SLUG, 8x down) are downregulated in LNT-229-rCPE cells.

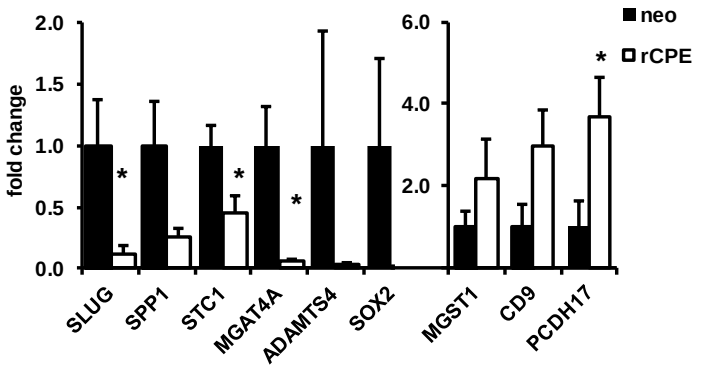

Figure 4.2.2 CPE modulates the expression of motility-associated genes. qRT-PCR of assorted genes we found to be differentially regulated by mRNA microarray epxression analysis in LNT229-rCPE vs.LNT-229-neo control cells and that are associated with cell motility. qRT-PCR was done in at least three LNT-229-rCPE or sibling neo-control cell clones (n>3, SEM, * $p < 0.05$).

Gene	Protein	pro/anti-migratory	Fold change in microarray (rCPE/neo)	Function	Association to signaling pathway
ADAMTS1	A Disintegrin And Metalloproteinase with Thrombospondin motifs 1	pro[90]	2.9 x down ($p<10^{-4}$)	Metalloproteinase, contributes to IGFII-mediated IGF1R phosphorylation and cellular migration in glioma cells, semaphorin 3C cleavage induced by ADAMTS1 promotes cell migration; marker for poor prognosis in glioma	FAK[91], integrin[92], TGF-β[93]
ADAMTS4	A Disintegrin And Metalloproteinase with Thrombospondin motifs 4	pro[94]	3.3 x down ($p<10^{-11}$)	Metalloproteinase, degradation of aggrecan, matrix degrading enzyme	FAK[95], integrin[92], TGF-β[96]
ARRDC3	Arrestin domain-containing 3	anti[97]	1,5 x up ($p<10^{-4}$)	Overexpression represses cancer cell proliferation, migration, invasion, growth in soft agar and in vivo tumorigenicity. Downregulation has	Integrin[97]

				the opposite effects; controls the cell surface adhesion molecule, beta-4 integrin, often epigenetically silenced	
CD9/MRP-1	Tetraspanin	anti[98]	3.5 up ($p<10^{-11}$)	Inhibits CD26 mediated enhancement of invasive potential of mesenthelioma; in glioma cells, knockdown of CD9 blocked PDGF stimulated migration	CDC42[99], FAK[100], integrin[101], STAT3[102]
CHL1/L1-CAM2	cell adhesion molecule L1-like	pro[103, 104]	5.1 x down ($p < 10^{-8}$)	Overexpressed in glioma stem cells.L1CAM stimulates glioma cell motility; Slug binding to on L1CAM promoters is essential for its induction by TGF-β	FAK[105], integrin[105], TGF-β[106]
PTGS2/COX-2	Cyclooxygenase 2	pro[107]	4.2 x down ($p < 10^{-6}$)	Enzyme involved in prostaglandin (including PGE2) biosynthesis, promotes glioma cell migration	STAT3[108], CDC42[109], FAK[110], integrin[111], TGF-β[112]
CTSD	Cathepsin D	pro[113]	1.7 x down ($p < 10^{-4}$)	Involved in cancer cell invasion. Cancer cell invasion is also induced by cathepsin B. Pro-cathepsin B is activated by cathepsin D	CDC42[114], STAT3[115]

CTSH	Cathepsin H	pro[116]	2,3 x down ($p < 10^{-4}$)	Induces glioma cell invasion, correlates with glioma malignancy, promotes hepatoma cell migration and invasion	Integrin[117]
ENPP2	Autotaxin	pro[118]	4 x down ($p < 10^{-10}$)	multifunctional phosphodiesterase, potent cell motility-stimulating factor in GBM, promotes MMP-3 production	STAT3[119], CDC42[120], FAK[121], integrin[122]
IGFBP7	Insulin-like growth factor binding protein 7	pro[123]	3.3 x down ($p<10^{-5}$)	Induces migration in glioma cells, IGFBP7 knockdown restores TGF-β induced EMT	TGF-β[124]
MGAT4A	N-Acetyl-Glucosamyl-Transferase IV A	pro[125]	3,2 x down ($p<10^{-9}$)	transfers GlcNAc in a specific linkage to N-glycans, upregulared in breast cancer tissue; high expression promotes invasion in choriocarcinoma	Integrin[126], TGF-β [127]
MGST1	Microsomal Glutathione-S-Transferase 1	[128]	5.4 x up ($p<10^{-12}$)	Involved in laminin-dependent migration in PC-12 cells, upregulated in glioma-derived glial progenitor cells, strongly downregulated in LTBP-/- mice	TGF-β [129]
MST4	member of the	pro[130]	13.2 x down	Involved in cell migration; promotes	

	Sterile 20 serine/threonine kinase family		($p<10^{-13}$)	hepatocellular carcinoma epithelial-mesenchymal transition	
PAK3	p21 protein activated kinase 3	pro[131]	1.98 x down ($p < 10^{-5}$)	stimulate cell migration and anchorage-independent growth	CDC42[132], FAK[133], integrin[134]
PCDH17	Procadherin 17	anti[135]	4.7 up ($p<10^{-11}$)	Inhibits cell migration and invasion of esophageal squamous cell carcinoma, silenced in many cancers, regulates actin dynamics; loss promotes metastasis and invasion in hepatocellular carcinoma cells	Integrin
PPARG	Peroxisome Proliferator-Activated Receptor γ	anti[136]	1.9 x up ($p<10^{-6}$)	PPARγ agonists block glioma motility and invasiveness	TGF-β [137], STAT3[138],
PTPRD	Protein Tyrosine Phosphatase, Receptor Type, D	anti[139, 140]	3.2 fold up ($p<10^{-7}$)	Loss in high grade GBM, reintroduction enhances cell adhesion of GBM cells, suppresses cancer cell migration	STAT3[139]

PXDN	Peroxidasin	pro[141]	8.7 down ($p<10^{-13}$)	regulator of cell plasticity and extracellular matrix remodeling; glioma endothelial marker gene, upregulated in tumor vasculature extracellular matrix	Integrin[142]
SDC2	Syndecan-2	pro[143]	2.7 down ($p<10^{-9}$)	Promotes membrane protrusion and migration; involved in cell adhesion; induces cell migration and invasion in human colon and pancreatic cancer cells	CDC42[144], FAK[145], integrin[143], TGF-β [146]
SNAI2	Slug	pro[28]	8.0 x down ($p < 10^{-8}$)	Transcription factor involved in the epithelial to mesenchymal (EMT) transition	STAT3[147], CDC42[148], Integrin[148], TGF-β[149]
SPP1	Osteopontin (OPN)	pro[150]	10.1 x down ($p<10^{-7}$)	Matricellular protein, promotes glioma cell migration and invasion	STAT3[151], CDC42/Rho[152], FAK[153], Integrin[153], TGF-β[154]

SOX2	SRY-box 2	pro[155]	2.6 x down ($p<10^{-4}$)	Stem cell marker	STAT3[147], TGF-β[156]
STC1	Stanniocalcin-1	pro[157]	1.6 x down ($p = 0.004$)	Secreted glycoprotein, biomarker of glioma progression, hypoxia-dependent migration factor in glioma	FAK[158], TGF-β[159]
TGFBR2	TGF-β Receptor Type II	pro[160]	1.9 x down ($p < 10^{-5}$)	Receptor for TGF-β, promotes migration in glioma cells	integrin[161],FAK [161] TGF-β[160]
ZFPM2/FOG-2	Zinc Finger Protein, FOG Family Member 2	pro[162]	2.3 x down ($p < 10^{-9}$)	Involved in post-mitotic neuronal migration, found to interact with STAT3 in liver	STAT3[163]

Table 4.2.1 Differentially regulated genes found by mRNA micro-array expression analysis and qRT-PCR that are known to be involved in processes regulating cell motility, and their association to motility-modulating signaling pathways.

Changes in expression of genes written in bold (LNT229-rCPE versus LNT-229-neo cells) were validated by qRT-PCR in at least three different clonal cell sublines (Figure 4.2.2).

In the past years many miRNAs have been discovered that are involved in cancer progression or in the regulation of cell motility and metastasis [164-168]. By miRNA microarray expression analysis of LNT-229rCPE- versus LNT-229-neo cells, followed by IPA and miR-target gene analysis, we identified 8 miRNAs (FDR > 0.05) that target differentially expressed RNAs (Table 4.2.2). Hsa-miR-182-5p (2.3 x up) targets SNAI2/SLUG and Hsa-miR-130a-3p (2.6 x down) targets PPARG and ZFPM2, both upregulated in LNT-229-rCPE cells. A further IPA analysis also demonstrates that the differentially expressed miRNAs we identified were also either directly or indirectly connected to the motility-associated signaling pathways mentioned above (Table 4.2.2).

miRNA	Fold change of miRNA expression in microarray analysis (rCPE vs. neo)	FDR	Putative miRNA targets differentially regulated and involved in migration	Fold change of target gene expression (rCPE vs. neo) depicted by microarray analysis	Association to signaling pathways
hsa-miR-199a-3p	25 x up ($p = 1 \times 10^{-7}$)	2.23×10^{-4}	PTGS2 MET	4.2 x down ($p = 4.7 \times 10^{-6}$) 1.5 x down ($p = 2.2 \times 10^{-4}$)	FAK, Integrin, TGF-β, CDC42
hsa-miR-182-5p	2.3 x up ($p = 2.9 \times 10^{-4}$)	2.89×10^{-2}	SNAI2[169] MITF	8.0 x down ($p = 1.6 \times 10^{-9}$) 2.0 x down ($p = 4.3 \times 10^{-5}$)	FAK, PAK, TGF-β, CDC42, STAT3
hsa-miR-140-5p	3.2 x up ($p = 1.97 \times 10^{-7}$)	3.27×10^{-4}	SOX2[170] TGFBR1[171]	2.6 x down ($p = 3.2 \times 10^{-5}$) 1.2 x down ($p = 1 \times 10^{-2}$)	PAK, Integrin, TGF-β, CDC42

hsa-miR-130a-3p	2.6 x down ($p = 3.3 \times 10^{-4}$)	3.,12 x 10^{-2}	PPARG[172, 173] ZFPM2	1.9 x up ($p = 2.5 \times 10^{-7}$) 2.3 x up ($p = 8.8 \times 10^{-10}$)	FAK, PAK, Integrin, TGF-β, CDC42, STAT3
hsa-miR-106b-5p	2.2 x up ($p = 2.47\ 10^{-5}$)	6.6 x 10^{-3}	TGFBR2	1.9 x down ($p = 5 \times 10^{-5}$)	FAK, TGF-β, CDC42, STAT3
hsa-miR-30e-3p	4 x up ($p = 4.2 \times 10^{-4}$)	3.5 x 10^{-2}	WDR44	1.8 x down ($p = 9.5 \times 10^{-6}$)	Integrin, TGF-β
hsa-miR-25-3p	2.2 x up ($p = 1.7 \times 10^{-5}$)	5.57 x 10^{-3}	FBXW7	1,6 x down ($p = 6{,}5 \times 10^{-5}$)	FAK, PAK, Integrin, TGF-β, CDC42, STAT3
hsa-let-7d-5p	1.5 x down $p = 1.3 \times 10^{-4}$)	1.56 x 10^{-2}	KRAS ITGB3	1.4 x up ($p = 4.5 \times 10^{-5}$) 1.8 x up ($p = 3 \times 10^{-5}$)	FAK, PAK, Integrin, TGF-β, CDC42, STAT3

Table 4.2.2 miRNA and their putative targets that are differentially expressed in LNT-229-rCPE versus LNT-229-neo cells.

4.3 CPE regulates the expression of SNAI2/SLUG

In the microarray expression analysis, and validated by qRT-PCR, we have found SNAI2/SLUG, known to be a pro-migratory and pro-invasive transcription factor in epithelial tumors, as one prominent mRNA being downregulated in LNT-229-rCPE cells. For this we tested whether this is also true for SLUG protein. Reduced amounts of SLUG protein were detectable in all rat and human CPE-overexpressing established glioma cell lines as well as in the low passage primary glioma cells we tested (Figure 4.3.1). Consistently, in Tu-140 cells, showing higher basal CPE expression, but no basal SNAI2/SLUG expression, SNAI2/SLUG was re-expressed at both mRNA and protein level after siRNA-mediated knockdown of CPE (Figure 4.3.2, this experiment was performed by E. Ilina, Goethe University, Frankfurt).

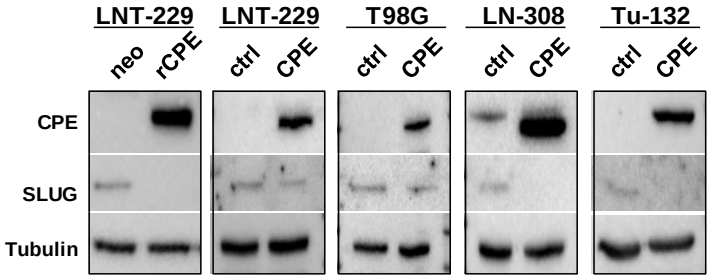

Figure 4.3.1 SLUG expression in CPE-overexpressing GBM cell lines. Immunoblot detection of CPE and SLUG in CPE-overexpressing and control LNT-229, T98G, LN-308 and Tu-132 cells. Tubulin was used as a loading control. (n = 3, one representative experiment is shown).

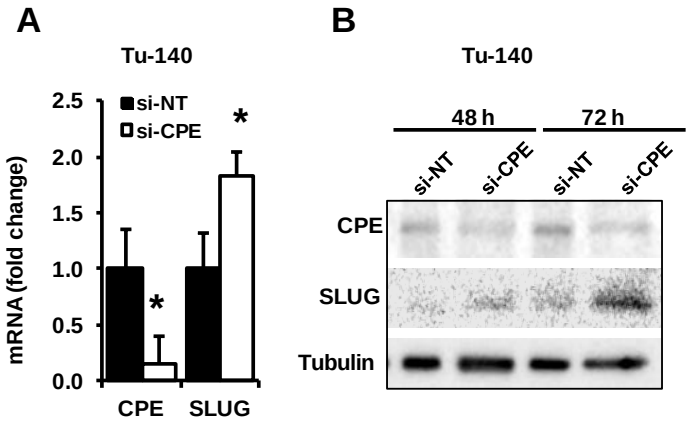

Figure 4.3.2 SLUG expression in TU-140 primary glioma cells after siRNA mediated knockdown of CPE. **A**. qRT-PCR analysis of CPE and SLUG mRNA in Tu-140 cells 48 h after siRNA transfection (si-NT, no-target siRNA; n=3, SD) **B.** Immunoblot detection of SLUG and CPE protein expression in Tu-140 cells 48 h or 72 h after siRNA-mediated knockdown of CPE. (n=3, one representative experiment is shown). Experiments performed by E. Ilina, Goethe University, Frankfurt. * $p < 0,05$.

We therefore tested whether glioma cell migration is modulated by SNAI2/SLUG. Adenovirus-based transient overexpression of SLUG induces migration whereas siRNA-mediated knockdown of SNAI2/SLUG reduces glioma cell migration (Figure 4.3.3).

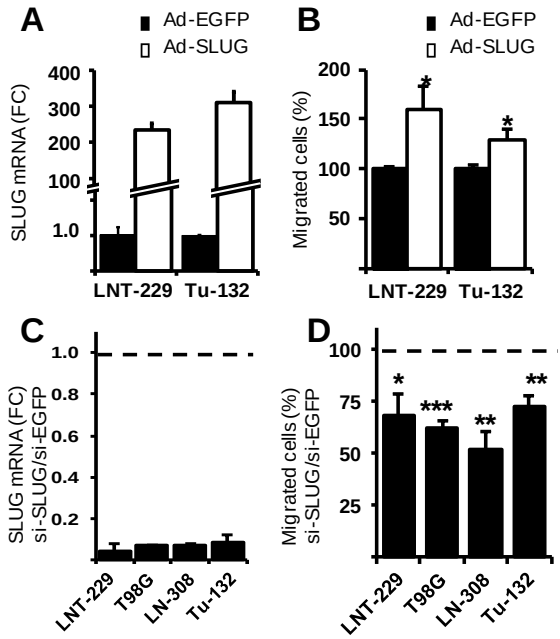

Figure 4.3.3 SLUG expression positively correlates with glioma cell migration. A. qRT-PCR of SLUG mRNA in LNT-229 and Tu-132 cells 48h after adenoviral infection with Ad-SLUG-GFP or Ad-EGFP. **B.** Migration of glioma cells infected as in A, analyzed with transwell migration chambers (FC, fold change; n=3, SEM). **C.** qRT-PCR of SLUG mRNA in glioma cells 48h after siRNA transfection with either SLUG (si-SLUG) or EGFP (si-EGFP) specific siRNA. The dashed line indicates the level of SLUG mRNA in siEGFP-transfected cells. **D.** Migration of glioma cells after siRNA-mediated knockdown of SLUG as described in C, analyzed with transwell migration chambers. The dashed line represents the amount of migrated cells in si-EGFP transfected cells (n=3, SEM).

It has been recently described that elevated SNAI2/SLUG correlates with the expression or activity of matrix metalloproteinases in several cancers [174]. Reduced expression of MMP-2 was detectable in LNT-229 and T98G cell lines that basically express MMP-2. MMP-2 is known to be activated by a complex containing MT1-MMP/MMP-14 and TIMP-2 [175]. With the exception of LN-308 cells, reduced levels of MT1-MMP/MMP-14 and TIMP-2 were detected in CPE-overexpressing cell lines (Figure 4.3.4).

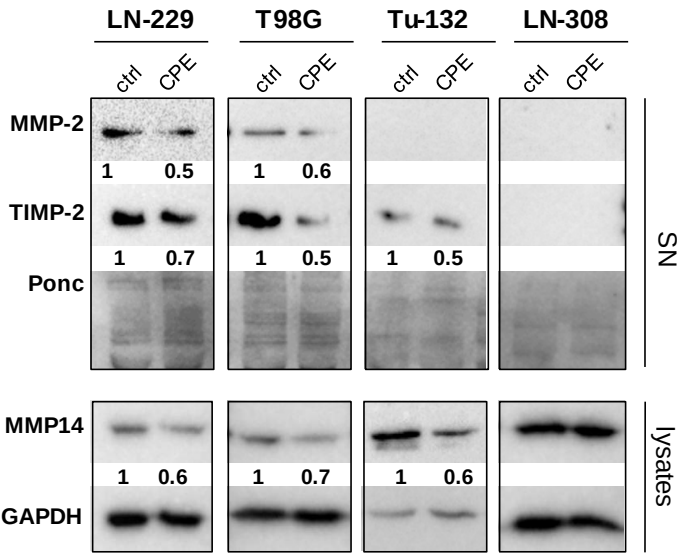

Figure 4.3.4 CPE modulates MMPs levels.
Immunoblot detection of MMP-2, TIMP-2 and MMP-14 in CPE-overexpressing and control LNT-229, T98G, Tu-132 and LN-308 cells. Values indicates the change in protein expression (MMP-2, n=2; TIMP-2, n=2; MMP-14, n=3) normalized to GAPDH for cytoplasmic proteins or to Ponceau S staining for secreted proteins.

4.4 The effects of CPE on the expression of SLUG and on glioma cell migration are transmitted by ERK1/2

It has been shown in hippocampus neurons [70] and in HCC cells [78] that CPE acts through ERK1/2. Therefore we tested whether ERK1/2 phosphorylation was altered in both rat and human CPE-overexpressing cells to verify if this applies to glioma cells, too. We found enhanced ERK1/2 phosphorylation in LNT-229 and Tu-132 CPE-overexpressing cells (Figure 4.4.1).

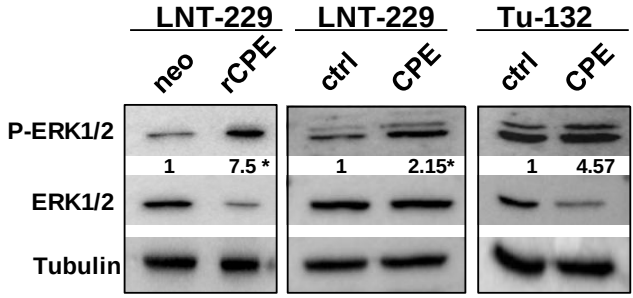

Figure 4.4.1 Overexpression of CPE is paralleled by enhanced ERK1/2 phosphorylation. Immunoblot detection of P-ERK1/2 and total ERK1/2 in CPE-overexpressing and control LNT-229 and Tu-132 cells. Values indicate the upregulation of P-ERK1/2 (signal intensity P-ERK1/2 / ERK1/2; n=3, one representative experiment is shown, * $p < 0.05$).

To verify whether ERK1/2 activation is at least partially responsible for CPE-mediated SLUG downregulation, we used the MEK inhibitor U0126 to inhibit ERK1/2 activity. SLUG expression was increased more prominently in U0126-treated CPE-overexpressing cells (Figure 4.4.2 B). In accordance, U0126 abolished the anti-migratory effects of CPE. Migration in CPE-overexpressing cells treated with U0126 reaches the basal level of migration of the respective control cells in both LNT-229 (either rat ot human) cells and in Tu-132 primary cells (Figure 4.4.2 C,D), while U0126 did not induce significant changes in control cells.

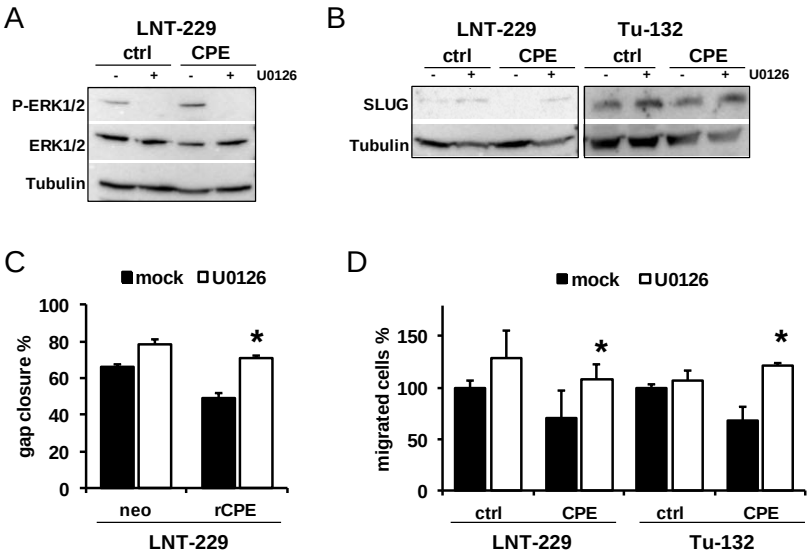

Figure 4.4.2 U0126 abolished CPE-mediated SLUG downregulation and induces cell migration.

A Immunoblot detection of P-ERK1/2 in LNT-229 and Tu-132 CPE-overexpressing and control cells treated with U0126 (10 µM, 24 h; n=3, one representative immunoblot is shown). **B** Immunoblot detection of SLUG in CPE-overexpressing and control LNT-229 and Tu-132 cells cultured in the absence or presence of U0126 (10 µM, 24 h; n=3, one representative immunoblot is shown). **C,D** Cell migration was analyzed by the scratch assay (C) and transwell migration assay (D) in rCPE-overexpressing and control neo LNT-229 (C) or in human CPE-overexpressing and control LNT-229 and Tu-132 cells (D) cultured in the absence (mock) or presence of U0126 (10 µM; n=3, SEM, * $p < 0,05$).

We were also interested to determine the upstream cell surface receptor by which CPE transmits its function into the intracellular compartment. Since it is known that EGFR phosphorylation is one main activator of ERK1/2 [176], we investigated whether sCPE could influence the phosphorylation and therefore activity of the EGFR. For this we cultivated LNT-229 cells in conditioned medium derived from control or CPE-overexpressing LNT-229 (either rat or human). We did not found any changes in P-EGFR after cultivation of the cells in sCPE-containing medium in both models tested, indicating that activation of the EGFR is not the responsible for enhanced ERK1/2 phosphorylation in CPE-overexpressing cells (Figure 4.4.3).

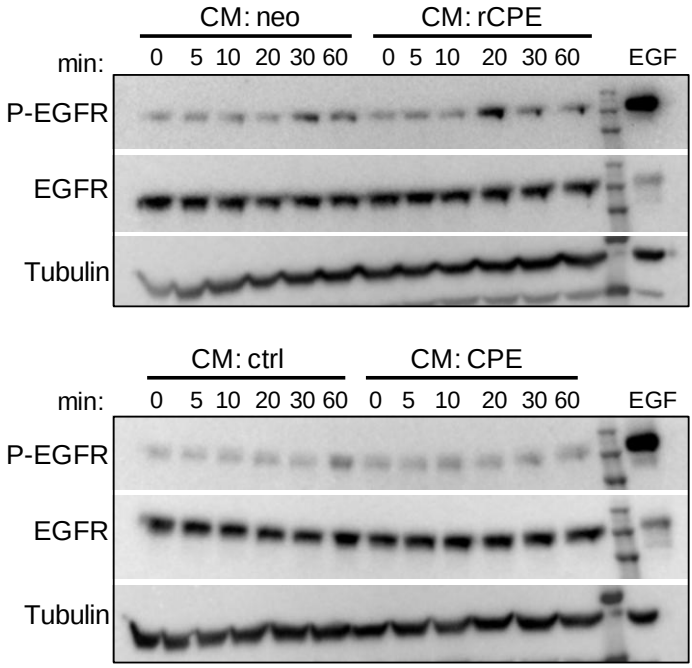

Figure 4.4.3 sCPE does not lead to enhanced phosphorylation of the EGFR.
Immunoblot detection of P-EGFR and total EGFR in LNT-229 cells cultivated for increasing time periods in conditioned medium generated from ctrl or CPE-overexpressing LNT-229 cells either rat or human CPE (n=2, one single experiment is shown).

4.5 CPE mediated downregulation of SLUG occurs independent from STAT3

It is known that SLUG expression can be also regulated by the activation of STAT3. Since many mRNAs we found to be differentially expressed in LNT-229-rCPE cells are associated to the STAT3 signaling pathway, we also analyzed STAT3 phosphorylation.

Reduced protein levels of P-STAT^{S727} were only detectable in LNT-229-rCPE cells, but in none of the human CPE overexpressing cell lines indicating either a clonal effect in LNT-229-rCPE cells or a species-specific effect of rat CPE (Figure 4.5.1 A). STAT3 inhibition using the STAT3 inhibitor S3I-201 reduced migration in LNT-229-neo cells but had no further effect on cell migration in LNT-229-rCPE cells (Figure 4.5.1 C).

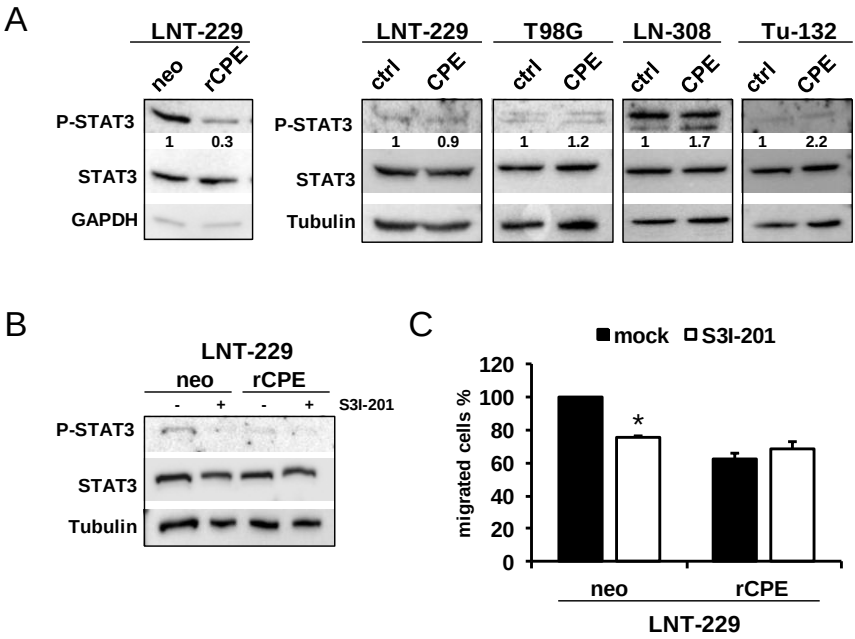

Figure 4.5.1 Effects of CPE on the phosphorylation of STAT3. A Immunoblot detection of P-STAT3^{S727}and total STAT3 in rat or human CPE-overexpressing and control glioma cells. Values indicate the changes in the signal density of P-STAT3 compared to total STAT3. (n=3, one representative experiment is shown). **B** Immunoblot detection of P-STAT3 in LNT-229 rCPE-overexpressing and control neo cells treated 24h with S3I-201 (10 μM). (n=3, one representative immunoblot is shown). **C** Cell migration was analyzed using the scratch migration assay in rCPE-overexpressing and control neo LNT-229 cells treated with or without (mock) S3I-201 (10 μM; n=3, SEM; *p< 0,05).

4.6 Effects of CPE on glioma therapeutic treatment options

Despites all efforts that have been ventured in GBM therapy research in the last decades, the median patient survival is still short. Therefore, novel adjuvant treatment options that can be used in parallel to the standard therapy (chemoradiotherapy) are necessary. In this regard we tested the effects of standard GBM therapy (irradiation and TMZ chemotherapy), if used in combination with the overexpression of CPE. Using the colony formation assay (Figure 4.6.1), we detected the outgrowth of glioma cell colonies from single cells, which is supposed to be the mechanism behind tumor recurrence after single cells escape after therapy. As shown in Figure 4.6.1, the number of colonies derived from CPE-overexpressing cells was lower compared to control neo cells and it was further reduced when cells where treated with TMZ and exposed to radiation, indicating that (at least rat) CPE overexpression alone reduces the clonal survival of glioma cells. Besides, CPE works in synergy with GBM standard therapy.

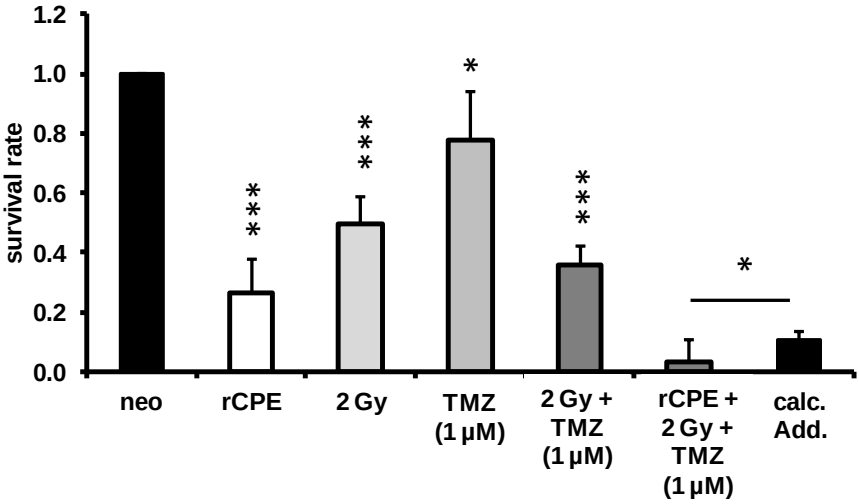

Figure 4.6.1 Effects of CPE on colony formation.
Colony formation assay in LNT-229-neo control and LNT-229-rCPE-overexpressing cells pre-treated with or without TMZ and/or irradiation (n=4, SD, * $p < 0.05$, *** $p < 0.005$).

In order to consider a translational application of CPE, we evaluated whether *in vivo* the CPE-mediated anti-migratory effect or reduced clonal survival we observed *in vitro* was associated to the survival of glioma bearing mice. For this we implanted control or CPE-overexpressing LNT-229 (either rat or human), and LN-308-ctrl or LN-308-CPE cells into the right striatum of NMRI nude mice. We monitored the influence of tumor development and growth by weight loss and neurological symptom. Mice were sacrificed if neurological symptoms and/or cachexia were observed and Kaplan-Meier survival curves were produced (Figure 4.6.2). Mice harboring tumors derived from CPE-overexpressing cells showed prolonged survival compared to mice harboring control tumors. The prolongation in survival was significant for LNT-229-CPE tumors (both rat and human CPE), while only a trend was observed in LN-308 tumors. We exemplarily analyzed tumor growth by MRI in 2 animals per group at different time points after tumor cell implantation (Figure 4.6.3), but did not observe any substantial difference in the tumor size between mice bearing control tumors or CPE-overexpressing tumor. Due to the small group size, it is only speculative to say that CPE did not influence tumor growth.

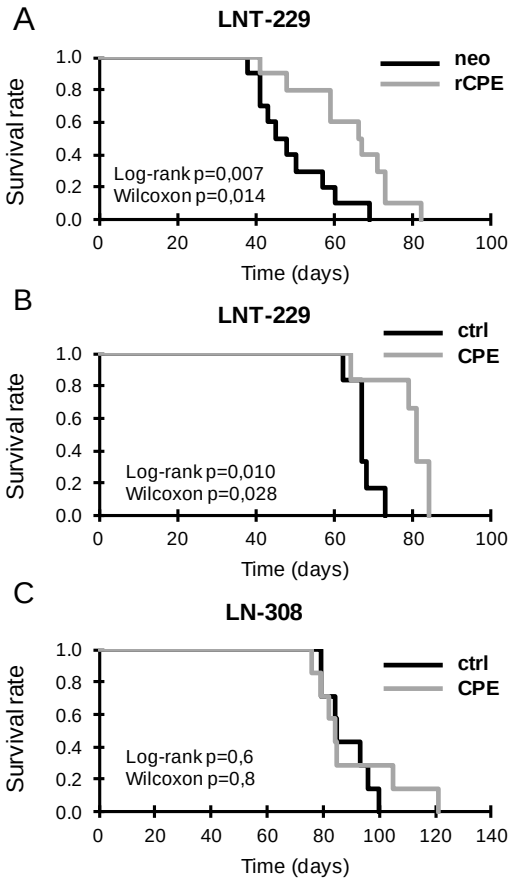

Figure 4.6.2 Kaplan-Meier survival curves of GBM bearing NMRI nude mice. A. Survival of animals bearing LNT-229-rCPE or LNT-229-neo xenografts. (summary of two independent experiments, n=10); **B.** LNT-229-CPE or LNT-229-ctrl (n=6); **C.** LN-308-CPE or LN-308-ctrl xenografts (n=7).

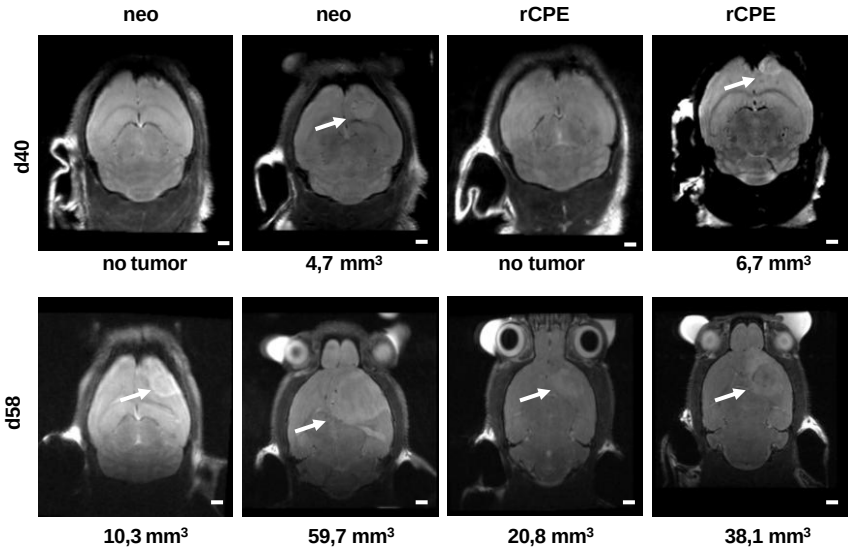

Figure 4.6.3 MRI of mice harboring LNT-229-rCPE or LNT-229-neo tumors

MRI images of mice brains at different time points after tumor cells implantation. Manually calculated tumor volumes are indicated below the images. Arrows point to the tumors locations.

5. DISCUSSION

Glioblastoma is the most malignant brain tumor, mainly because of its infiltrative growth, its immunosuppression, its resistance towards cells death but also because of its ability to adapt to the tumor microenvironment. One mechanism which includes both adaptation and invasion actuated by glioma cells is the switch between the proliferative or migratory phenotype depending on the circumstances, leading to the "Grow or Go" behavior of glioma cells. It has been described by Höring et al. [51] that one of the factors modulating this process is a secreted version of Carboxypeptidase E. In particular, in a rat CPE-overexpressing model, sCPE enhanced glioma cell proliferation whereas migration was reduced.

Main foci of this thesis were to test whether CPE is a "Grow or Go" switch factor in GBM and how CPE transmits its function. Therefore we used LNT-229 rat CPE-overexpressing clonal cell lines generated by Höring [51] as well as produced stable human CPE-overexpressing primary and established GBM cell lines.

The pro-proliferative role of CPE has been investigated in other cancer entities, like CRC, in which CPE-mediated

downregulation of $p21^{WAF1}$ led to enhanced proliferation [79]. For glioma cells, increased proliferation was only detectable in LNT-229-rCPE cells as previously described by Höring [51], while this effect was absent or only marginal in human CPE-overexpressing glioma cells (Figure 4.1.3), even though the cell cycle regulator $p21^{WAF1}$ was downregulated in all (both rat and human) CPE-overexpressing cells (Figure 4.1.2). On the contrary, cell migration was significantly reduced in all (rat and human) CPE-overexpressing primary cells as well as in established GBM cell lines. Consistently, siRNA-mediated downregulation of CPE in highly CPE-expressing Tu-140 glioma primary cells induced cell motility (Figure 4.1.4).

These data indicate that CPE exert its function on GBM cells through the modulation of cell migration whereas the effects of CPE on proliferation seemed to be species-specific.

Rat and human CPE are highly homologous with a 96% identity and 98% similarity in the amino acid (AA) sequence and even a total conservation of the Zn-carboxypeptidase domain. Therefore the enzymatic activity is not different between rat and human CPE [57]. Besides, a correct procession and maturation of CPE might be conserved for both species, since the penta-arginine

sequence ($RRRRR_{42}$) also shows 100% homology. Changes in the AA sequence occur in proximity of the prohormone sorting signal binding site. One could speculate that the latter might play a major role in the functional differences between rat and human CPE and make the prohormone sorting signal binding site as the putative domain responsible for different effects of rat and human CPE on cell growth.

In this study we focused to evaluate how CPE transmits its anti-migratory function in glioma cells. Our findings as well as knowledge from the literature suggest that CPE modulates, beside the ERK1/2, also the AKT and/or WNT signaling pathway as it has been described for other tumor and non-tumor cells such as HCC, CRC, pheochromocytoma cells or hypocampal neurons [70, 78, 177, 178]. However, which pathways or which factors are involved in CPE-mediated effects on GBM cell migration has not been elucidated in detail. In this regard, changes in the expression of motility-associated genes have been analyzed as well as signaling cascades that are modulated by CPE have been investigated.

Using mRNA and miRNA microarray chip technology in LNT-229-rCPE cells and LNT-229-neo cells, followed by quantitative RT-PCR validation of mRNA expression and

IPA, we investigated CPE-mediated changes in gene expression and its impact of motility-associated signaling cascades. We found that 1065 mRNA were differentially expressed and at least 100 genes were either directly or indirectly connected to the regulation of cell motility (Supplementary Table 1). In addition, eight miRNA, in combination with their reverse expressed targets, are differentially regulated in LNT-229-rCPE cells (Table 4.2.2). Many of the motility-associated genes and all miRNAs showed a connection to motility-associated pathways integrating TGF-β, CDC42, PAK, FAK, STAT3 and integrin. IPA demonstrated an enrichment of differentially expressed mRNAs associated to the above mentioned signaling cascades (Figure 4.2.1, Table 4.2.2).

After intensive validation of microarray data by qRT-PCR we identified genes known to regulate cell motility that are significantly differentially expressed (Figure 4.2.2): *procaherin-17* (PCDH17, 4.7 x in LNT-229-rCPE) inhibits cell migration and invasion of esophageal squamous cell carcinoma, it is silenced in many cancers and regulates actin dynamics [135]. *Stanniocalcin-1* (STC1, 1.6 x down in LNT-229-rCPE), a secreted glycoprotein, is a biomarker of glioma progression and it is involved in hypoxia-dependent migration in glioma [157]. *Osteopontin*

(OPN/SPP1, 10.1 x down in LNT-229-rCPE), a matricellular protein, promotes glioma and stem cell migration and invasion through a variety of pathways [150-154], and *A disintegrin and metalloprotease with trombospondin motifs* (ADAMTS4, 3.3 x down in LNT-229-rCPE) and *N-Acetyl-Glucosamyl-Transferase IV A* (MGAT4A, 3.2 x down in LNT-229-rCPE) are involved in invasive processes. ADAMTS4 leads to the degradation of aggrecan. In an oligodendroglioma model, ADAMTS4 it is responsible for cell invasion through aggrecan-rich extracellular matrices [179] whereas MGAT4A transfers a N-acetylglucosamine (GlcNAc) group to N-glycans, this resulting in increased GlcNAc-N-glycan branches on integrin β1 and promotion of invasion of choriocarcinoma cells [125].

One prominent downregulated gene is *snail family zink finger 2* (SNAI2/SLUG, 8x down in LNT-229-rCPE), which has been linked to the more malignant, more invasive and migratory mesenchymal phenotype of gliomas as well as to pro-tumorigenic processes of many other cancers [28, 180, 181]. SNAI2/SLUG expression is either directly or indirectly regulated by CPE, since it is downregulated in all CPE-overexpressing primary and established GBM cells (Figure 4.3.1), whereas

downregulation of CPE by siRNA led to enhanced SLUG expression in Tu-140 cells (Figure 4.3.2). SNAI2/SLUG modulates cell migration through different mechanisms. After TGF-β administration, SLUG binds to both promoters of the *cell adhesion molecule with homology* gene (CHL/L1-CAM-2; 5.1 x down in LNT-229-rCPE) this way inducing L1-CAM expression [106]. L1-CAMs are described to enhance glioma cell motility and invasion and correlate with FAK activity [182]. In glioma cells, CPE-mediated anti-migratory effects seemed to be directly dependent on SLUG, since exogenous overexpression of SLUG significantly enhanced migration whereas its knockdown significantly mitigated glioma cell migration to about 60% of the control, the same percentage of reduction we observed by CPE overexpression. This suggests that the CPE-mediated downregulation of SLUG might be a central component to reduce cell motility in CPE-overexpressing glioma cells (Figure 4.3.3).

During glioma invasion different MMPs can be activated to destroy the extracellular matrix and make it more accessible for invading cells. Therefore we tested MMP expression and found reduced levels of MMP-2, MT1-MMP/MMP-14 and TIMP-2 in those human CPE-

overexpressing glioma cells that express these enzymes (Figure 4.3.4).

In a recent study in breast cancer cells, metabolic changes induced during epithelial-to-mesenchymal transition (EMT) have been elucidated [183]. EMT-derived breast cancer cells show enhanced expression EMT proteins including SNAI2/SLUG. Besides, they display an increase in aerobic glycolysis at the expenses of the pentose phosphate pathway (PPP) and glycogen synthesis. This metabolic switch is mediated by increased glucose uptake and lactate production, through the upregulation of glucose transporters (GLUT3), lactate dehydrogenases (LDHA) and lactate transporters (MCT4). In a parallel study (data in publication) in collaboration with Prof. Dr. Michel Mittelbronn and Elena I. Ilina (Neuropathology, Goethe-University Frankfurt), we investigated the metabolic changes in CPE-overexpressing GBM cells, the same cells that showed lower levels of SLUG and lesser cell migration. We found that GLUT3, LDHA and MCT4 expression was reduced in CPE-overexpressing cells and observed a shift to the utilization of the PPP pathway, instead of using aerobic glycolysis. However, whether these changes are caused directly by CPE or by the CPE-

mediated downregulation of SNAI2/SLUG has not been investigated so far.

Another purpose of this study was to decipher the signaling pathway(s) by which CPE mediates its effects on GBM cell motility. IPA analysis and literature research performed on the differentially regulated genes, as mentioned before, highlights the putative involvement of TGF-β, CDC42, PAK, FAK, STAT3 and integrin signaling pathways in the anti-migratory function of CPE. In hippocampal neurons [70] and HCC cells [78], CPE acts through ERK1/2. Therefore we decided to focus on the ERK1/2 pathway to verify if this applies on glioma cells, too. We analyzed if ERK1/2 activation affects SLUG expression and modulates GBM cell migration. We observed enhanced ERK1/2 phosphorylation in both rat and human CPE-overexpressing LNT-229 and in Tu-132-CPE primary GBM cells, indicating that enhanced activation of ERK1/2 in CPE-overexpressing cells correlates with reduced SLUG levels and lesser migration (Figure 4.4.1). Typically, the ERK1/2 pathway is associated with increased migration, especially in the context of EMT that follows the EGFR/Src/ERK/SLUG signaling axis [184]. Controversially it has been described that ERK1/2 inhibition by U0126 did not cause any changes on cell

migration in some glioma cell lines [185, 186]. Indeed, we detected no major changes in glioma cell migration after inhibition of ERK1/2 activation glioma control cells. Interestingly, inhibition of CPE-mediated ERK1/2 phosphorylation with U0126 in CPE-overexpressing cells was able to abolish the CPE-mediated downregulation of SNAI2/SLUG as well as the CPE-mediated reduction of migration and restore the same amount of SLUG and migration we observed in control cells (Figure 4.4.2).

We were interested in identify upstream receptors that might be responsible for the sCPE mediated phosphorylation of ERK1/2. First our collaborator E. I. Ilina analyzed the phosphorylation of a panel of surface receptors using a membrane-base assay and found slightly elevated levels of P-EGFR in LNT-229-rCPE cells. However, immunoblot analyses done in our lab to show EGFR phosphorylation in parental glioma cells treated with sCPE-containing cell supernatants generated from CPE-overexpressing cells did not confirm these results (Figure 4.4.3).

Recent studies showed that ERK1/2 can also regulate the P-STAT3^{S727}, this way modulating STAT3 tyrosine phosphorylation which is necessary for its nuclear transport and DNA binding as a transcription factor [190]. Since

many of the differentially expressed genes, including SNAI2/SLUG, are targets of the STAT3 pathway, we also analyzed STAT3 phosphorylation. STAT3^{S727} phosphorylation was only reduced in LNT-29-rCPE cells. No changes in P-STAT ^{S727} were observed in human-CPE overexpressing cells. Although STAT3 inhibition was able to abolish the anti-migratory effects of CPE effects in LNT-229-neo control cells, there was no effect on the migration in LNT-229-rCPE cells (Figure 4.5.1), suggesting that reduced P-STAT ^{S727} in LNT-229-rCPE cells was either a clonal effect or was a result of a species-specific function of CPE.

Our data indicate that CPE might act through a still unknown receptor or binding partner that leads to activation or inhibition of several signaling cascades. One of these signaling pathways integrates the activation of ERK1/2 to ultimately reduce SLUG expression and migration of GBM cells. It will be a challenge for the future to identify the upstream factors that functionally lead to the activation of ERK1/2, finally resulting in an altered expression of motility-regulating genes in CPE expressing glioma cells.

Besides, considering all known and putative functions of CPE, it could be suggested that also other mechanisms

could be involved in its anti-migratory effect. It has been recently described that CPE obstructs the β-catenin pathway, inhibits the secretion and activity of Wnt3a and forms aggregates with it into non soluble cellular fraction [80]. However, the role of CPE in Wnt3a-mediated cell migration has not been investigated so far. Taking into account the enzymatic activity of CPE and its role in protein sorting, and also knowing that sCPE is not active in the extracellular space due to a neutral pH in this compartment, it is still possible that during the secretion process CPE modulates the vesicles contents leading to a rearrangement of the secretome that might contain secretable, motility-regulating factors.

Another hypothesis how CPE can also transmit its anti-migratory effects is the knowledge that, during or after exocytosis, membrane bound CPE (mCPE), by interaction with ARF6, is recycled back to the TGN [67]. ARF6 mediates Rac1 activation and actin remodeling, necessary for glioma invasion. Inhibition of ARF6 in GBM cells reduces cell migration [191]. By CPE overexpression also the mCPE levels might be elevated. Therefore ARF6 is recruited by mCPE and it is not able anymore to exert its pro-migratory function.

Considering that CPE, among 311 proteases, is the only protease that has been found to be downregulated in GBM specimens [192], we decided to investigate the role of CPE from a more clinical point of view and to evaluate whether the anti-migratory effects induced by CPE we observed *in vitro* is associated to the survival of GBM bearing mice *in vivo*.

We evaluated whether CPE influences the effects of GBM standard therapy *in vitro* and found that CPE acts in synergy with GBM standard therapy regarding the reduction to the outgrowth of tumor cells clones from single tumor cell (Figure 4.6.1).

This makes sCPE a possible marker protein to predict the outcome of glioma radiochemotherapy in GBM patients or even a putative candidate for an adjuvant treatment of GBM. In orthotopic GBM mouse models we showed that mice harboring tumors derived from CPE-overexpressing cells lived longer than mice harboring control tumors (Figure 4.6.2). This indicates that CPE-overexpressing glioma cells produce either lesser infiltrative/invasive growing tumors or that a lesser amount of cells expressing CPE survive or grow up if they settle, after implantation, as single cells in the brains micro-milieu.

6. CONCLUSIONS

The data presented in this study clarify some of the mechanisms by which CPE, and especially sCPE, mitigates GBM cell migration. In particular we identified SNAI2/SLUG and the ERK1/2 pathway, among other cell motility-associated genes and cascades, to be mediators of the anti-migratory effects of CPE. In addition, we proved that CPE provides a beneficial role by enhancing the effect of radiochemotherapy at least *in vitro*. In a mouse glioma model, overexpression of CPE prolonged the survival *in vivo*.

Nevertheless, further investigation will be necessary to completely understand the mechanism of action of CPE and the feasibility to use this protein as a therapeutic agent in the treatment of malignant glioma.

7. SUPPLEMENTARIES

Supplementary Table 1: Differential expression of 100 cell motility-associated genes in LNT-229-rCPE versus LNT-229-neo control cells detected by microarray expression analysis.

UPREGULATED GENES				
Gene	**Protein**	**Fold change (rCPE vs neo)**	**p-value**	**FDR**
IL15	interleukin 15	5.46	1.09E-10	1.19E-07
MGST1	Microsomal Glutathione-S-Transferase 1	5.42	5.22E-13	2.52E-09
PCDH17	protocadherin 17	4.67	1.81E-11	3.82E-08
CD9	CD9 molecule	3.53	4.63E-11	6.42E-08
DACH1	dachshund homolog 1 (Drosophila)	3.49	2.62E-10	2.26E-07
ALX1	ALX homeobox 1	3.40	1.56E-09	8.29E-07
SCG2	secretogranin II	3.08	5.22E-06	4.70E-04
LIN28B	lin-28 homolog B (C. elegans)	2.81	5.90E-09	2.36E-06
MSR1	macrophage scavenger receptor 1	2.60	2.86E-08	8.07E-06
PTPRD	protein tyrosine phosphatase, receptor type, D	2.59	1.26E-10	1.35E-07
PAPPA	pregnancy-associated plasma protein A, pappalysin 1	2.52	1.35E-06	1.65E-04

CCL2	chemokine (C-C motif) ligand 2	2.36	7.81E-05	3.67E-03
BDKRB2	bradykinin receptor B2	2.34	2.02E-05	1.31E-03
ZFPM2	zinc finger protein, multitype 2	2.30	8.88E-10	5.45E-07
EPS8	epidermal growth factor receptor pathway substrate 8	2.23	1.70E-05	1.14E-03
CTSK	cathepsin K	2.22	1.05E-07	2.16E-05
FOXM1	forkhead box M1	2.22	1.29E-04	5.37E-03
EREG	epiregulin	2.18	2.45E-06	2.66E-04
UBD	ubiquitin D	2.10	7.48E-05	3.54E-03
MGP	matrix Gla protein	2.10	9.87E-09	3.55E-06
BHLHE41	basic helix-loop-helix family, member e41	2.05	1.80E-06	2.06E-04
SERPINB5	serpin peptidase inhibitor, clade B (ovalbumin), member 5	2.01	1.39E-07	2.73E-05
TNFAIP8	tumor necrosis factor, alpha-induced protein 8	2.00	8.21E-07	1.10E-04
PODXL	podocalyxin-like	1.98	1.82E-08	5.65E-06
PRKCD	protein kinase C, delta	1.96	2.65E-06	2.84E-04
BMP2	bone morphogenetic protein 2	1.94	6.13E-05	3.04E-03
PPARG	peroxisome proliferator-activated receptor gamma	1.89	2.57E-07	4.45E-05
ITGB3	integrin, beta 3 (platelet glycoprotein IIIa, antigen CD61)	1.87	3.07E-05	1.81E-03

FNBP1L	formin binding protein 1-like	1.86	7.19E-05	3.43E-03
KDM5A	lysine (K)-specific demethylase 5A	1.73	5.48E-06	4.86E-04
GBP1	guanylate binding protein 1, interferon-inducible	1.73	4.30E-05	2.34E-03
TPM1	tropomyosin 1 (alpha)	1.70	1.78E-06	2.04E-04
LOXL2	lysyl oxidase-like 2	1.68	5.40E-07	7.94E-05
SERPINA 5	serpin peptidase inhibitor, clade A (alpha-1 antiproteinase, antitrypsin), member 5	1.67	6.89E-07	9.75E-05
DNAJB4	DnaJ (Hsp40) homolog, subfamily B, member 4	1.67	3.68E-06	3.70E-04
CSF2RA	colony stimulating factor 2 receptor, alpha	1.64	6.83E-06	5.72E-04
ZEB1	zinc finger E-box binding homeobox 1	1.63	6.59E-05	3.21E-03
MFI2	antigen p97 (melanoma associated)	1.63	1.53E-06	1.82E-04
KCNN3	potassium intermediate/small conductance calcium-activated channel, subfamily N, 3	1.62	2.01E-05	1.31E-03
SLC12A6	solute carrier family 12 (potassium/chloride transporters), member 6	1.62	3.96E-06	3.87E-04

PTPRF	protein tyrosine phosphatase, receptor type, F	1.57	6.96E-06	5.81E-04
INADL	InaD-like (Drosophila)	1.57	1.07E-04	4.86E-03
NOTCH2	notch 2	1.56	9.16E-06	7.09E-04
ARRDC3	arrestin domain containing 3	1.55	7.88E-05	3.69E-03
FERMT1	fermitin family member 1	1.55	2.30E-05	1.44E-03
PRKAR2A	protein kinase, cAMP-dependent, regulatory, type II, alpha	1.54	1.83E-04	7.01E-03
CSPG4	chondroitin sulfate proteoglycan 4	1.53	3.57E-06	3.60E-04
NFKBIA	nuclear factor of kappa light polypeptide gene enhancer in B-cells inhibitor, alpha	1.53	5.81E-05	2.92E-03
GAB1	GRB2-associated binding protein 1	1.52	7.82E-06	6.28E-03
TGFA	transforming growth factor, alpha	1.51	5.46E-06	4.86E-04
DOWNREGULATED GENES				
Gene	**Protein**	**Fold change (rCPE vs neo)**	**p-value**	**FDR**
MST4	serine/threonine protein kinase MST4	-13.23	1.38E-14	1.59E-10
SPP1	secreted phosphoprotein 1	-10.18	7.60E-08	1.71E-05
PXDN	perxoidasin	-8.73	1.61E-13	1.21E-09

SNAI2	snail homolog 2 (Drosophila)	-8.04	1.68E-09	8.74E-07
CHL1	cell adhesion molecule with homology to L1CAM (close homolog of L1)	-5.15	9.35E-09	3.42E-06
A2M	alpha-2-macroglobulin	-4.58	7.38E-07	1.02E-04
MAP7D3	MAP7 domain containing 3	-4.32	4.34E-09	1.82E-06
PTGS2/COX2	prostaglandin-endoperoxide synthase 2 , cyclooxigenase-2	-4.20	4.70E-06	4.32E-04
ENPP2	ectonucleotide pyrophosphatase/ phosphodiesterase 2	-4.06	3.87E-10	2.90E-07
GDF15	growth differentiation factor 15	-3.62	1.99E-04	7.44E-03
DKK1	dickkopf 1 homolog (Xenopus laevis)	-3.42	2.38E-04	8.55E-03
IGFBP7	insulin-like growth factor bindung protein 7	-3.35	1.30E-06	7.78E-05
ADAMTS4	ADAM metallopeptidase with thrombospondin type 4	-3.32	2.13E-11	3.88E-08
MGAT4A	N-Acetyl-Glucosamyl-Transferase IV A	-3.23	1.64E-10	1.61E-07
LPAR1	lysophosphatidic acid receptor 1	-2.96	2.21E-07	3.94E-05
ADAMTS1	ADAM metallopeptidase with thrombospondin type 1 motif, 1	-2.90	6.77E-08	1.56E-05

FHL1	four and a half LIM domains 1	-2.82	1.83E-07	3.42E-05
SDC2	syndecan 2	-2.74	9.42E-09	3.42E-06
SOX2	SRY (sex determining region Y)-box 2	-2.66	3.29E-05	1.92E-03
IFIT2	interferon-induced protein with tetratricopeptide repeats 2	-2.60	5.24E-07	1.61E-04
EHF	ets homologous factor	-2.35	1.08E-04	4.72E-03
CTSH	cathepsin H	-2.32	2.33E-09	1.12E-06
KITLG	KIT ligand	-2.22	4.31E-07	6.74E-05
ANGPTL 1	angiopoietin-like 1	-2.18	4.95E-07	7.45E-05
TLR4	toll-like receptor 4	-2.16	2.96E-06	3.12E-04
MITF	microphthalmia-associated transcription factor	-2.00	4.36E-05	2.36E-03
LYN	v-yes-1 Yamaguchi sarcoma viral related oncogene homolog	-1.99	7.03E-05	3.37E-03
PAK3	p21 protein (CDC42/Rac)-activated kinase 3	-1.98	2.15E-06	2.38E-04
TGFBR2	transforming growth factor, beta receptor II (70/80kDa)	-1.94	5.07E-05	2.65E-03
TIAM1	T-cell lymphoma invasion and metastasis 1	-1.85	4.27E-06	4.04E-04
SLC12A2	solute carrier family 12 (sodium/potassium/chloride transporters),	-1.84	9.87E-06	7.50E-04

	member 2			
WDR44	WD repeat domain 44	-1.82	9.52E-06	7.30E-04
CTSD	cathepsin D	-1.75	1.47E-04	5.90E-03
FGF7	fibroblast growth factor 7	-1.73	8.05E-06	6.43E-04
STC1	stanniocalcin 1	-1.67	4.01E-02	2.81E-01
SH3PXD 2B	SH3 and PX domains 2B	-1.65	1.03E-05	7.77E-04
RHOU	ras homolog family member U	-1.64	9.48E-06	7.30E-04
CLU	clusterin	-1.63	1.03E-06	1.34E-04
S100B	S100 calcium binding protein B	-1.62	4.94E-05	2.61E-03
LGALS3	lectin, galactoside-binding, soluble, 3	-1.61	1.66E-05	1.12E-03
FKBP1A	FK506 binding protein 1A, 12kDa	-1.60	4.74E-05	2.52E-03
WWOX	WW domain containing oxidoreductase	-1.60	3.78E-06	3.74E-04
CTGF	connective tissue growth factor	-1.57	8.06E-05	3.75E-03
XIAP	X-linked inhibitor of apoptosis	-1.55	1.84E-04	7.04E-03
NOV	nephroblastoma overexpressed	-1.54	8.41E-05	3.87E-03
MET	met proto-oncogene (hepatocyte growth factor receptor)	-1.53	2.27E-04	8.31E-03
IFNAR1	interferon (alpha, beta and omega) receptor 1	-1.52	5.81E-05	2.92E-03
AZGP1	alpha-2-glycoprotein 1, zinc-binding	-1.52	5.42E-05	2.78E-03

SIM2	single-minded homolog 2 (Drosophila)	-1.50	2.90E-04	9.76E-03
WARS	tryptophanyl-tRNA synthetase	-1.50	2.04E-05	1.32E-03

8. REFERENCES

1. Walsh, K.M., H. Ohgaki, and M.R. Wrensch, *Epidemiology.* Handb Clin Neurol, 2016. **134**: p. 3-18.
2. Ohgaki, H. and P. Kleihues, *Genetic pathways to primary and secondary glioblastoma.* Am J Pathol, 2007. **170**(5): p. 1445-53.
3. Boele, F.W., et al., *Attitudes and preferences toward monitoring symptoms, distress, and quality of life in glioma patients and their informal caregivers.* Support Care Cancer, 2016. **24**(7): p. 3011-22.
4. Sterckx, W., et al., *The impact of a high-grade glioma on everyday life: a systematic review from the patient's and caregiver's perspective.* Eur J Oncol Nurs, 2013. **17**(1): p. 107-17.
5. Louis, D.N., et al., *The 2007 WHO classification of tumours of the central nervous system.* Acta Neuropathol, 2007. **114**(2): p. 97-109.
6. Stupp, R., et al., *Radiotherapy plus concomitant and adjuvant temozolomide for glioblastoma.* N Engl J Med, 2005. **352**(10): p. 987-96.
7. Louis, D.N., et al., *The 2016 World Health Organization Classification of Tumors of the Central Nervous System: a summary.* Acta Neuropathol, 2016. **131**(6): p. 803-20.
8. Zou, P., et al., *IDH1/IDH2 mutations define the prognosis and molecular profiles of patients with gliomas: a meta-analysis.* PLoS One, 2013. **8**(7): p. e68782.
9. Redzic, J.S., T.H. Ung, and M.W. Graner, *Glioblastoma extracellular vesicles: reservoirs of*

potential biomarkers. Pharmgenomics Pers Med, 2014. **7**: p. 65-77.
10. Phillips, H.S., et al., *Molecular subclasses of high-grade glioma predict prognosis, delineate a pattern of disease progression, and resemble stages in neurogenesis.* Cancer Cell, 2006. **9**(3): p. 157-73.
11. Verhaak, R.G., et al., *Integrated genomic analysis identifies clinically relevant subtypes of glioblastoma characterized by abnormalities in PDGFRA, IDH1, EGFR, and NF1.* Cancer Cell, 2010. **17**(1): p. 98-110.
12. Aldape, K., et al., *Glioblastoma: pathology, molecular mechanisms and markers.* Acta Neuropathol, 2015. **129**(6): p. 829-48.
13. Kalman, B., et al., *Epidermal growth factor receptor as a therapeutic target in glioblastoma.* Neuromolecular Med, 2013. **15**(2): p. 420-34.
14. Seger, R. and E.G. Krebs, *The MAPK signaling cascade.* FASEB J, 1995. **9**(9): p. 726-35.
15. Crespo, I., et al., *Molecular and Genomic Alterations in Glioblastoma Multiforme.* Am J Pathol, 2015. **185**(7): p. 1820-33.
16. Eisele, G. and M. Weller, *Targeting apoptosis pathways in glioblastoma.* Cancer Lett, 2013. **332**(2): p. 335-45.
17. Paolillo, M., M. Serra, and S. Schinelli, *Integrins in glioblastoma: Still an attractive target?* Pharmacol Res, 2016. **113**(Pt A): p. 55-61.
18. van Nimwegen, M.J. and B. van de Water, *Focal adhesion kinase: a potential target in cancer therapy.* Biochem Pharmacol, 2007. **73**(5): p. 597-609.

19. Bigarella, C.L., et al., *ARHGAP21 modulates FAK activity and impairs glioblastoma cell migration.* Biochim Biophys Acta, 2009. **1793**(5): p. 806-16.
20. Okura, H., et al., *A role for activated CDC42 in glioblastoma multiforme invasion.* Oncotarget, 2016.
21. Imada, K. and W.J. Leonard, *The Jak-STAT pathway.* Mol Immunol, 2000. **37**(1-2): p. 1-11.
22. Birner, P., et al., *STAT3 tyrosine phosphorylation influences survival in glioblastoma.* J Neurooncol, 2010. **100**(3): p. 339-43.
23. Priester, M., et al., *STAT3 silencing inhibits glioma single cell infiltration and tumor growth.* Neuro Oncol, 2013. **15**(7): p. 840-52.
24. Massaous, J. and A. Hata, *TGF-beta signalling through the Smad pathway.* Trends Cell Biol, 1997. **7**(5): p. 187-92.
25. Wick, W., M. Platten, and M. Weller, *Glioma cell invasion: regulation of metalloproteinase activity by TGF-beta.* J Neurooncol, 2001. **53**(2): p. 177-85.
26. Wang, M., et al., *The expression of matrix metalloproteinase-2 and -9 in human gliomas of different pathological grades.* Brain Tumor Pathol, 2003. **20**(2): p. 65-72.
27. Iser, I.C., et al., *The Epithelial-to-Mesenchymal Transition-Like Process in Glioblastoma: An Updated Systematic Review and In Silico Investigation.* Med Res Rev, 2016.
28. Yang, H.W., et al., *SNAI2/Slug promotes growth and invasion in human gliomas.* BMC Cancer, 2010. **10**: p. 301.
29. Qi, S., et al., *ZEB2 mediates multiple pathways regulating cell proliferation, migration, invasion,*

and apoptosis in glioma. PLoS One, 2012. **7**(6): p. e38842.
30. Platten, M., et al., *Transforming growth factors beta(1) (TGF-beta(1)) and TGF-beta(2) promote glioma cell migration via Up-regulation of alpha(V)beta(3) integrin expression.* Biochem Biophys Res Commun, 2000. **268**(2): p. 607-11.
31. Tania, M., M.A. Khan, and J. Fu, *Epithelial to mesenchymal transition inducing transcription factors and metastatic cancer.* Tumour Biol, 2014. **35**(8): p. 7335-42.
32. Liu, Y., et al., *Multidimensional analysis of gene expression reveals TGFB1I1-induced EMT contributes to malignant progression of astrocytomas.* Oncotarget, 2014. **5**(24): p. 12593-606.
33. Brat, D.J., et al., *Pseudopalisades in glioblastoma are hypoxic, express extracellular matrix proteases, and are formed by an actively migrating cell population.* Cancer Res, 2004. **64**(3): p. 920-7.
34. Du, R., et al., *HIF1alpha induces the recruitment of bone marrow-derived vascular modulatory cells to regulate tumor angiogenesis and invasion.* Cancer Cell, 2008. **13**(3): p. 206-20.
35. Zheng, J., *Energy metabolism of cancer: Glycolysis versus oxidative phosphorylation (Review).* Oncol Lett, 2012. **4**(6): p. 1151-1157.
36. Nduom, E.K., M. Weller, and A.B. Heimberger, *Immunosuppressive mechanisms in glioblastoma.* Neuro Oncol, 2015. **17 Suppl 7**: p. vii9-vii14.
37. Schonberg, D.L., et al., *Brain tumor stem cells: Molecular characteristics and their impact on therapy.* Mol Aspects Med, 2014. **39**: p. 82-101.
38. Carlsson, S.K., S.P. Brothers, and C. Wahlestedt, *Emerging treatment strategies for glioblastoma*

multiforme. EMBO Mol Med, 2014. **6**(11): p. 1359-70.
39. Miletic, H., et al., *Anti-VEGF therapies for malignant glioma: treatment effects and escape mechanisms.* Expert Opin Ther Targets, 2009. **13**(4): p. 455-68.
40. Taylor, T.E., F.B. Furnari, and W.K. Cavenee, *Targeting EGFR for treatment of glioblastoma: molecular basis to overcome resistance.* Curr Cancer Drug Targets, 2012. **12**(3): p. 197-209.
41. Thomas, A.A., M.S. Ernstoff, and C.E. Fadul, *Immunotherapy for the treatment of glioblastoma.* Cancer J, 2012. **18**(1): p. 59-68.
42. Wollmann, G., K. Ozduman, and A.N. van den Pol, *Oncolytic virus therapy for glioblastoma multiforme: concepts and candidates.* Cancer J, 2012. **18**(1): p. 69-81.
43. Ene, C.I. and E.C. Holland, *Personalized medicine for gliomas.* Surg Neurol Int, 2015. **6**(Suppl 1): p. S89-95.
44. Giese, A., et al., *Dichotomy of astrocytoma migration and proliferation.* Int J Cancer, 1996. **67**(2): p. 275-82.
45. Hatzikirou, H., et al., *'Go or grow': the key to the emergence of invasion in tumour progression?* Math Med Biol, 2012. **29**(1): p. 49-65.
46. Böttger, K., et al., *Investigation of the Migration/Proliferation Dichotomy and its Impact on Avascular Glioma Invasion.* Mathematical Modelling of Natural Phenomena, 2012. **7**(1): p. 105-135.
47. Kathagen-Buhmann, A., et al., *Glycolysis and the pentose phosphate pathway are differentially associated with the dichotomous regulation of*

glioblastoma cell migration versus proliferation. Neuro Oncol, 2016. **18**(9): p. 1219-29.
48. Huber, S.M., et al., *Ionizing radiation, ion transports, and radioresistance of cancer cells.* Front Physiol, 2013. **4**: p. 212.
49. Godlewski, J., et al., *MicroRNA-451 regulates LKB1/AMPK signaling and allows adaptation to metabolic stress in glioma cells.* Mol Cell, 2010. **37**(5): p. 620-32.
50. Tan, X., et al., *The CREB-miR-9 negative feedback minicircuitry coordinates the migration and proliferation of glioma cells.* PLoS One, 2012. **7**(11): p. e49570.
51. Horing, E., et al., *The "go or grow" potential of gliomas is linked to the neuropeptide processing enzyme carboxypeptidase E and mediated by metabolic stress.* Acta Neuropathol, 2012. **124**(1): p. 83-97.
52. Fricker, L.D. and S.H. Snyder, *Enkephalin convertase: purification and characterization of a specific enkephalin-synthesizing carboxypeptidase localized to adrenal chromaffin granules.* Proc Natl Acad Sci U S A, 1982. **79**(12): p. 3886-90.
53. Steiner, D.F., *The proprotein convertases.* Curr Opin Chem Biol, 1998. **2**(1): p. 31-9.
54. Naggert, J.K., et al., *Hyperproinsulinaemia in obese fat/fat mice associated with a carboxypeptidase E mutation which reduces enzyme activity.* Nat Genet, 1995. **10**(2): p. 135-42.
55. Reznik, S.E. and L.D. Fricker, *Carboxypeptidases from A to z: implications in embryonic development and Wnt binding.* Cell Mol Life Sci, 2001. **58**(12-13): p. 1790-804.

56. Rawlings, N.D. and A.J. Barrett, *Evolutionary families of metallopeptidases.* Methods Enzymol, 1995. **248**: p. 183-228.
57. Cawley, N.X., et al., *New roles of carboxypeptidase E in endocrine and neural function and cancer.* Endocr Rev, 2012. **33**(2): p. 216-53.
58. Jung, Y.K., et al., *Structural characterization of the rat carboxypeptidase-E gene.* Mol Endocrinol, 1991. **5**(9): p. 1257-68.
59. Lee, T.K., et al., *An N-terminal truncated carboxypeptidase E splice isoform induces tumor growth and is a biomarker for predicting future metastasis in human cancers.* J Clin Invest, 2011. **121**(3): p. 880-92.
60. Song, L. and L. Fricker, *Processing of procarboxypeptidase E into carboxypeptidase E occurs in secretory vesicles.* J Neurochem, 1995. **65**(1): p. 444-53.
61. Fricker, L.D. and L. Devi, *Posttranslational processing of carboxypeptidase E, a neuropeptide-processing enzyme, in AtT-20 cells and bovine pituitary secretory granules.* J Neurochem, 1993. **61**(4): p. 1404-15.
62. Loh, Y.P., C.R. Snell, and D.R. Cool, *Receptor-mediated targeting of hormones to secretory granules: role of carboxypeptidase E.* Trends Endocrinol Metab, 1997. **8**(4): p. 130-7.
63. Chanat, E. and W.B. Huttner, *Milieu-induced, selective aggregation of regulated secretory proteins in the trans-Golgi network.* J Cell Biol, 1991. **115**(6): p. 1505-19.
64. Cool, D.R., et al., *Carboxypeptidase E is a regulated secretory pathway sorting receptor:*

genetic obliteration leads to endocrine disorders in Cpe(fat) mice. Cell, 1997. **88**(1): p. 73-83.
65. Normant, E. and Y.P. Loh, *Depletion of carboxypeptidase E, a regulated secretory pathway sorting receptor, causes misrouting and constitutive secretion of proinsulin and proenkephalin, but not chromogranin A.* Endocrinology, 1998. **139**(4): p. 2137-45.
66. Greene, D., B. Das, and L.D. Fricker, *Regulation of carboxypeptidase E. Effect of pH, temperature and Co2+ on kinetic parameters of substrate hydrolysis.* Biochem J, 1992. **285 (Pt 2)**: p. 613-8.
67. Arnaoutova, I., et al., *Recycling of Raft-associated prohormone sorting receptor carboxypeptidase E requires interaction with ARF6.* Mol Biol Cell, 2003. **14**(11): p. 4448-57.
68. Jin, K., et al., *Altered expression of the neuropeptide-processing enzyme carboxypeptidase E in the rat brain after global ischemia.* J Cereb Blood Flow Metab, 2001. **21**(12): p. 1422-9.
69. Zhou, A., et al., *Altered biosynthesis of neuropeptide processing enzyme carboxypeptidase E after brain ischemia: molecular mechanism and implication.* J Cereb Blood Flow Metab, 2004. **24**(6): p. 612-22.
70. Cheng, Y., N.X. Cawley, and Y.P. Loh, *Carboxypeptidase E/NFalpha1: a new neurotrophic factor against oxidative stress-induced apoptotic cell death mediated by ERK and PI3-K/AKT pathways.* PLoS One, 2013. **8**(8): p. e71578.
71. Qin, X.Y., et al., *carboxypeptidase E-DeltaN, a neuroprotein transiently expressed during development protects embryonic neurons against*

glutamate neurotoxicity. PLoS One, 2014. **9**(11): p. e112996.
72. Jeffrey, K.D., et al., *Carboxypeptidase E mediates palmitate-induced beta-cell ER stress and apoptosis.* Proc Natl Acad Sci U S A, 2008. **105**(24): p. 8452-7.
73. Ge, X., et al., *Interpreting expression profiles of cancers by genome-wide survey of breadth of expression in normal tissues.* Genomics, 2005. **86**(2): p. 127-41.
74. Du, J., B.P. Keegan, and W.G. North, *Key peptide processing enzymes are expressed by breast cancer cells.* Cancer Lett, 2001. **165**(2): p. 211-8.
75. Murthy, S.R., K. Pacak, and Y.P. Loh, *Carboxypeptidase E: elevated expression correlated with tumor growth and metastasis in pheochromocytomas and other cancers.* Cell Mol Neurobiol, 2010. **30**(8): p. 1377-81.
76. Liu, T., et al., *Detection of a microRNA signal in an in vivo expression set of mRNAs.* PLoS One, 2007. **2**(8): p. e804.
77. Zhou, K., et al., *Overexpression of CPE-DeltaN predicts poor prognosis in colorectal cancer patients.* Tumour Biol, 2013. **34**(6): p. 3691-9.
78. Murthy, S.R., et al., *Carboxypeptidase E promotes cancer cell survival, but inhibits migration and invasion.* Cancer Lett, 2013. **341**(2): p. 204-13.
79. Liang, X.H., et al., *Upregulation of CPE promotes cell proliferation and tumorigenicity in colorectal cancer.* BMC Cancer, 2013. **13**: p. 412.
80. Skalka, N., et al., *Carboxypeptidase E (CPE) inhibits the secretion and activity of Wnt3a.* Oncogene, 2016.
81. Fan, S., et al., *Silencing of carboxypeptidase E inhibits cell proliferation, tumorigenicity, and*

metastasis of osteosarcoma cells. Onco Targets Ther, 2016. **9**: p. 2795-803.
82. Ishii, N., et al., *Frequent co-alterations of TP53, p16/CDKN2A, p14ARF, PTEN tumor suppressor genes in human glioma cell lines.* Brain Pathol, 1999. **9**(3): p. 469-79.
83. Benjamini, Y. and Y. Hochberg, *Controlling the False Discovery Rate: A Practical and Powerful Approach to Multiple Testing.* Journal of the Royal Statistical Society. Series B (Methodological), 1995. **57**(1): p. 289-300.
84. Bradford, M.M., *A rapid and sensitive method for the quantitation of microgram quantities of protein utilizing the principle of protein-dye binding.* Anal Biochem, 1976. **72**: p. 248-54.
85. Smith, P.K., et al., *Measurement of protein using bicinchoninic acid.* Anal Biochem, 1985. **150**(1): p. 76-85.
86. Feoktistova, M., P. Geserick, and M. Leverkus, *Crystal Violet Assay for Determining Viability of Cultured Cells.* Cold Spring Harb Protoc, 2016. **2016**(4): p. pdb prot087379.
87. Webb, J.L., *Effect of more than one inhibitor.* Enzyme and metabolic inhibitors, 1963. **1**: p. 66-79.
88. Naumann, U., et al., *Chimeric tumor suppressor 1, a p53-derived chimeric tumor suppressor gene, kills p53 mutant and p53 wild-type glioma cells in synergy with irradiation and CD95 ligand.* Cancer Res, 2001. **61**(15): p. 5833-42.
89. He, T.C., et al., *A simplified system for generating recombinant adenoviruses.* Proc Natl Acad Sci U S A, 1998. **95**(5): p. 2509-14.
90. Martino-Echarri, E., et al., *Relevance of IGFBP2 proteolysis in glioma and contribution of the*

extracellular protease ADAMTS1. Oncotarget, 2014. **5**(12): p. 4295-304.
91. Chen, S.Z., et al., *The miR-181d-regulated metalloproteinase Adamts1 enzymatically impairs adipogenesis via ECM remodeling.* Cell Death Differ, 2016. **23**(11): p. 1778-1791.
92. Bridges, L.C. and R.D. Bowditch, *ADAM-Integrin Interactions: potential integrin regulated ectodomain shedding activity.* Curr Pharm Des, 2005. **11**(7): p. 837-47.
93. Le Bras, G.F., et al., *TGFbeta loss activates ADAMTS-1-mediated EGF-dependent invasion in a model of esophageal cell invasion.* Exp Cell Res, 2015. **330**(1): p. 29-42.
94. Held-Feindt, J., et al., *Matrix-degrading proteases ADAMTS4 and ADAMTS5 (disintegrins and metalloproteinases with thrombospondin motifs 4 and 5) are expressed in human glioblastomas.* Int J Cancer, 2006. **118**(1): p. 55-61.
95. Gilbert, H.T., et al., *Integrin - dependent mechanotransduction in mechanically stimulated human annulus fibrosus cells: evidence for an alternative mechanotransduction pathway operating with degeneration.* PLoS One, 2013. **8**(9): p. e72994.
96. Hopwood, B., et al., *Microarray gene expression profiling of osteoarthritic bone suggests altered bone remodelling, WNT and transforming growth factor-beta/bone morphogenic protein signalling.* Arthritis Res Ther, 2007. **9**(5): p. R100.
97. Draheim, K.M., et al., *ARRDC3 suppresses breast cancer progression by negatively regulating integrin beta4.* Oncogene, 2010. **29**(36): p. 5032-47.

98. Fabian, J., et al., *MYCN and HDAC5 transcriptionally repress CD9 to trigger invasion and metastasis in neuroblastoma.* Oncotarget, 2016.
99. Arnaud, M.P., et al., *CD9, a key actor in the dissemination of lymphoblastic leukemia, modulating CXCR4-mediated migration via RAC1 signaling.* Blood, 2015. **126**(15): p. 1802-12.
100. Powner, D., et al., *Tetraspanin CD9 in cell migration.* Biochem Soc Trans, 2011. **39**(2): p. 563-7.
101. Reyes, R., et al., *Different states of integrin LFA-1 aggregation are controlled through its association with tetraspanin CD9.* Biochim Biophys Acta, 2015. **1853**(10 Pt A): p. 2464-80.
102. Shi, Y., et al., *Tetraspanin CD9 stabilizes gp130 by preventing its ubiquitin-dependent lysosomal degradation to promote STAT3 activation in glioma stem cells.* Cell Death Differ, 2016.
103. Katic, J., et al., *Interaction of the cell adhesion molecule CHL1 with vitronectin, integrins, and the plasminogen activator inhibitor-2 promotes CHL1-induced neurite outgrowth and neuronal migration.* J Neurosci, 2014. **34**(44): p. 14606-23.
104. Kiefel, H., et al., *EMT-associated up-regulation of L1CAM provides insights into L1CAM-mediated integrin signalling and NF-kappaB activation.* Carcinogenesis, 2012. **33**(10): p. 1919-29.
105. Anderson, H.J. and D.S. Galileo, *Small-molecule inhibitors of FGFR, integrins and FAK selectively decrease L1CAM-stimulated glioblastoma cell motility and proliferation.* Cell Oncol (Dordr), 2016. **39**(3): p. 229-42.
106. Geismann, C., et al., *Binding of the transcription factor Slug to the L1CAM promoter is essential for*

transforming growth factor-beta1 (TGF-beta)-induced L1CAM expression in human pancreatic ductal adenocarcinoma cells. Int J Oncol, 2011. **38**(1): p. 257-66.
107. Wang, L., et al., *NFATc1 activation promotes the invasion of U251 human glioblastoma multiforme cells through COX-2.* Int J Mol Med, 2015. **35**(5): p. 1333-40.
108. Liu, X., et al., *Berberine Inhibits Invasion and Metastasis of Colorectal Cancer Cells via COX-2/PGE2 Mediated JAK2/STAT3 Signaling Pathway.* PLoS One, 2015. **10**(5): p. e0123478.
109. Bozza, W.P., et al., *RhoGDI deficiency induces constitutive activation of Rho GTPases and COX-2 pathways in association with breast cancer progression.* Oncotarget, 2015. **6**(32): p. 32723-36.
110. Lichtenstein, M.P., et al., *JNK/ERK/FAK mediate promigratory actions of basic fibroblast growth factor in astrocytes via CCL2 and COX2.* Neurosignals, 2012. **20**(2): p. 86-102.
111. Aggarwal, A., et al., *Expression of integrin alpha3beta1 and cyclooxygenase-2 (COX2) are positively correlated in human breast cancer.* BMC Cancer, 2014. **14**: p. 459.
112. Haidar, M., et al., *Transforming growth factor beta2 promotes transcription of COX2 and EP4, leading to a prostaglandin E2-driven autostimulatory loop that enhances virulence of Theileria annulata-transformed macrophages.* Infect Immun, 2015. **83**(5): p. 1869-80.
113. Rao, J.S., *Molecular mechanisms of glioma invasiveness: the role of proteases.* Nat Rev Cancer, 2003. **3**(7): p. 489-501.
114. Ohri, S.S., et al., *Depletion of procathepsin D gene expression by RNA interference: a potential*

therapeutic target for breast cancer. Cancer Biol Ther, 2007. **6**(7): p. 1081-7.
115. Hilfiker-Kleiner, D., et al., *A cathepsin D-cleaved 16 kDa form of prolactin mediates postpartum cardiomyopathy.* Cell, 2007. **128**(3): p. 589-600.
116. Sivaparvathi, M., et al., *Expression and the role of cathepsin H in human glioma progression and invasion.* Cancer Lett, 1996. **104**(1): p. 121-6.
117. Jevnikar, Z., et al., *Cathepsin H mediates the processing of talin and regulates migration of prostate cancer cells.* J Biol Chem, 2013. **288**(4): p. 2201-9.
118. Hoelzinger, D.B., et al., *Autotaxin: a secreted autocrine/paracrine factor that promotes glioma invasion.* J Neurooncol, 2008. **86**(3): p. 297-309.
119. Azare, J., et al., *Stat3 mediates expression of autotaxin in breast cancer.* PLoS One, 2011. **6**(11): p. e27851.
120. Jung, I.D., et al., *CDC42 and Rac1 are necessary for autotaxin-induced tumor cell motility in A2058 melanoma cells.* FEBS Lett, 2002. **532**(3): p. 351-6.
121. Fox, M.A., et al., *Phosphodiesterase-I alpha/autotaxin controls cytoskeletal organization and FAK phosphorylation during myelination.* Mol Cell Neurosci, 2004. **27**(2): p. 140-50.
122. Wu, T., et al., *Integrin-mediated cell surface recruitment of autotaxin promotes persistent directional cell migration.* FASEB J, 2014. **28**(2): p. 861-70.
123. Jiang, W., et al., *Insulin-like growth factor binding protein 7 mediates glioma cell growth and migration.* Neoplasia, 2008. **10**(12): p. 1335-42.
124. Watanabe, J., et al., *Role of IGFBP7 in Diabetic Nephropathy: TGF-beta1 Induces IGFBP7 via*

Smad2/4 in Human Renal Proximal Tubular Epithelial Cells. PLoS One, 2016. **11**(3): p. e0150897.
125. Niimi, K., et al., *High expression of N-acetylglucosaminyltransferase IVa promotes invasion of choriocarcinoma.* Br J Cancer, 2012. **107**(12): p. 1969-77.
126. Kunneken, K., et al., *Recombinant human laminin-5 domains. Effects of heterotrimerization, proteolytic processing, and N-glycosylation on alpha3beta1 integrin binding.* J Biol Chem, 2004. **279**(7): p. 5184-93.
127. Chen, Y.J., et al., *Hexosamine-Induced TGF-beta Signaling and Osteogenic Differentiation of Dental Pulp Stem Cells Are Dependent on N-Acetylglucosaminyltransferase V.* Biomed Res Int, 2015. **2015**: p. 924397.
128. Sobczak, M., et al., *Functional characteristic of PC12 cells with reduced microsomal glutathione transferase 1.* Acta Biochim Pol, 2010. **57**(4): p. 589-96.
129. Li, N., et al., *Altered beta1,6-GlcNAc branched N-glycans impair TGF-beta-mediated epithelial-to-mesenchymal transition through Smad signalling pathway in human lung cancer.* J Cell Mol Med, 2014. **18**(10): p. 1975-91.
130. Lin, Z.H., et al., *MST4 promotes hepatocellular carcinoma epithelial-mesenchymal transition and metastasis via activation of the p-ERK pathway.* Int J Oncol, 2014. **45**(2): p. 629-40.
131. Holderness Parker, N., et al., *p21-activated kinase 3 (PAK3) is an AP-1 regulated gene contributing to actin organisation and migration of transformed fibroblasts.* PLoS One, 2013. **8**(6): p. e66892.

132. Moorman, V.R., et al., *Dynamic and thermodynamic response of the Ras protein CDC42Hs upon association with the effector domain of PAK3.* J Mol Biol, 2014. **426**(21): p. 3520-38.
133. Bagrodia, S., et al., *A tyrosine-phosphorylated protein that binds to an important regulatory region on the cool family of p21-activated kinase-binding proteins.* J Biol Chem, 1999. **274**(32): p. 22393-400.
134. Allen, K.M., et al., *PAK3 mutation in nonsyndromic X-linked mental retardation.* Nat Genet, 1998. **20**(1): p. 25-30.
135. Haruki, S., et al., *Frequent silencing of protocadherin 17, a candidate tumour suppressor for esophageal squamous cell carcinoma.* Carcinogenesis, 2010. **31**(6): p. 1027-36.
136. Grommes, C., et al., *Inhibition of in vivo glioma growth and invasion by peroxisome proliferator-activated receptor gamma agonist treatment.* Mol Pharmacol, 2006. **70**(5): p. 1524-33.
137. Zhang, J., et al., *Correlation between TSP-1, TGF-beta and PPAR-gamma expression levels and glioma microvascular density.* Oncol Lett, 2014. **7**(1): p. 95-100.
138. Akasaki, Y., et al., *A peroxisome proliferator-activated receptor-gamma agonist, troglitazone, facilitates caspase-8 and -9 activities by increasing the enzymatic activity of protein-tyrosine phosphatase-1B on human glioma cells.* J Biol Chem, 2006. **281**(10): p. 6165-74.
139. Kim, J.E., et al., *STAT3 Activation in Glioblastoma: Biochemical and Therapeutic Implications.* Cancers (Basel), 2014. **6**(1): p. 376-95.

140. Navis, A.C., et al., *Protein tyrosine phosphatases in glioma biology.* Acta Neuropathol, 2010. **119**(2): p. 157-75.
141. Jayachandran, A., et al., *Identifying and targeting determinants of melanoma cellular invasion.* Oncotarget, 2016.
142. Hennigan, K., et al., *Eosinophil peroxidase activates cells by HER2 receptor engagement and beta1-integrin clustering with downstream MAPK cell signaling.* Clin Immunol, 2016. **171**: p. 1-11.
143. Choi, S., et al., *Syndecan-2 overexpression regulates adhesion and migration through cooperation with integrin alpha2.* Biochem Biophys Res Commun, 2009. **384**(2): p. 231-5.
144. Granes, F., et al., *Syndecan-2 induces filopodia by active CDC42Hs.* Exp Cell Res, 1999. **248**(2): p. 439-56.
145. Park, H., et al., *Focal adhesion kinase regulates syndecan-2-mediated tumorigenic activity of HT1080 fibrosarcoma cells.* Cancer Res, 2005. **65**(21): p. 9899-905.
146. Chen, L., C. Klass, and A. Woods, *Syndecan-2 regulates transforming growth factor-beta signaling.* J Biol Chem, 2004. **279**(16): p. 15715-8.
147. Gao, H., et al., *SOX2 Promotes the Epithelial to Mesenchymal Transition of Esophageal Squamous Cells by Modulating Slug Expression through the Activation of STAT3/HIF-alpha Signaling.* Int J Mol Sci, 2015. **16**(9): p. 21643-57.
148. Shields, M.A., et al., *Interplay between beta1-integrin and Rho signaling regulates differential scattering and motility of pancreatic cancer cells by snail and Slug proteins.* J Biol Chem, 2012. **287**(9): p. 6218-29.

149. Joseph, M.J., et al., *Slug is a downstream mediator of transforming growth factor-beta1-induced matrix metalloproteinase-9 expression and invasion of oral cancer cells.* J Cell Biochem, 2009. **108**(3): p. 726-36.
150. Lu, D.Y., et al., *Osteopontin increases heme oxygenase-1 expression and subsequently induces cell migration and invasion in glioma cells.* Neuro Oncol, 2012. **14**(11): p. 1367-78.
151. Behera, R., et al., *Activation of JAK2/STAT3 signaling by osteopontin promotes tumor growth in human breast cancer cells.* Carcinogenesis, 2010. **31**(2): p. 192-200.
152. Teramoto, H., et al., *Autocrine activation of an osteopontin-CD44-Rac pathway enhances invasion and transformation by H-RasV12.* Oncogene, 2005. **24**(3): p. 489-501.
153. Zou, C., et al., *Osteopontin promotes mesenchymal stem cell migration and lessens cell stiffness via integrin beta1, FAK, and ERK pathways.* Cell Biochem Biophys, 2013. **65**(3): p. 455-62.
154. Weber, C.E., et al., *Epithelial-mesenchymal transition, TGF-beta, and osteopontin in wound healing and tissue remodeling after injury.* J Burn Care Res, 2012. **33**(3): p. 311-8.
155. Hattermann, K., et al., *Stem cell markers in glioma progression and recurrence.* Int J Oncol, 2016. **49**(5): p. 1899-1910.
156. Weina, K., et al., *TGF-beta induces SOX2 expression in a time-dependent manner in human melanoma cells.* Pigment Cell Melanoma Res, 2016. **29**(4): p. 453-8.
157. Yoon, J.H., et al., *Proteomic analysis of hypoxia-induced U373MG glioma secretome reveals novel*

hypoxia-dependent migration factors. Proteomics, 2014. **14**(12): p. 1494-502.
158. Yeung, B.H. and C.K. Wong, *Stanniocalcin-1 regulates re-epithelialization in human keratinocytes.* PLoS One, 2011. **6**(11): p. e27094.
159. Ono, M., et al., *Mesenchymal stem cells correct inappropriate epithelial-mesenchyme relation in pulmonary fibrosis using stanniocalcin-1.* Mol Ther, 2015. **23**(3): p. 549-60.
160. Lu, Y., et al., *TGF-beta1 promotes motility and invasiveness of glioma cells through activation of ADAM17.* Oncol Rep, 2011. **25**(5): p. 1329-35.
161. Yoshimoto, T., et al., *Aggregatibacter actinomycetemcomitans outer membrane protein 29 (Omp29) induces TGF-beta-regulated apoptosis signal in human gingival epithelial cells via fibronectin/integrinbeta1/FAK cascade.* Cell Microbiol, 2016.
162. Kwan, K.Y., et al., *SOX5 postmitotically regulates migration, postmigratory differentiation, and projections of subplate and deep-layer neocortical neurons.* Proc Natl Acad Sci U S A, 2008. **105**(41): p. 16021-6.
163. Mei, S., et al., *MicroRNA-200c Promotes Suppressive Potential of Myeloid-Derived Suppressor Cells by Modulating PTEN and FOG2 Expression.* PLoS One, 2015. **10**(8): p. e0135867.
164. Chen, Q., et al., *MiR-19a promotes cell proliferation and invasion by targeting RhoB in human glioma cells.* Neurosci Lett, 2016. **628**: p. 161-6.
165. Chen, S., et al., *HLF/miR-132/TTK axis regulates cell proliferation, metastasis and radiosensitivity of glioma cells.* Biomed Pharmacother, 2016. **83**: p. 898-904.

166. Chen, X., et al., *MiR-129 triggers autophagic flux by regulating a novel Notch-1/ E2F7/Beclin-1 axis to impair the viability of human malignant glioma cells.* Oncotarget, 2016. **7**(8): p. 9222-35.
167. Fu, Q., et al., *An oncogenic role of miR-592 in tumorigenesis of human colorectal cancer by targeting Forkhead Box O3A (FoxO3A).* Expert Opin Ther Targets, 2016. **20**(7): p. 771-82.
168. Gu, J.J., et al., *MicroRNA-130b promotes cell proliferation and invasion by inhibiting peroxisome proliferator-activated receptor-gamma in human glioma cells.* Int J Mol Med, 2016. **37**(6): p. 1587-93.
169. Kouri, F.M., C. Ritner, and A.H. Stegh, *miRNA-182 and the regulation of the glioblastoma phenotype - toward miRNA-based precision therapeutics.* Cell Cycle, 2015. **14**(24): p. 3794-800.
170. Zhang, Y., et al., *Estrogen receptor alpha signaling regulates breast tumor-initiating cells by down-regulating miR-140 which targets the transcription factor SOX2.* J Biol Chem, 2012. **287**(49): p. 41514-22.
171. Yang, H., et al., *MicroRNA-140-5p suppresses tumor growth and metastasis by targeting transforming growth factor beta receptor 1 and fibroblast growth factor 9 in hepatocellular carcinoma.* Hepatology, 2013. **58**(1): p. 205-17.
172. Su, S., et al., *miR-142-5p and miR-130a-3p are regulated by IL-4 and IL-13 and control profibrogenic macrophage program.* Nat Commun, 2015. **6**: p. 8523.
173. Seufert, S., et al., *PPAR Gamma Activators: Off-Target Against Glioma Cell Migration and Brain Invasion.* PPAR Res, 2008. **2008**: p. 513943.

174. Lamouille, S., J. Xu, and R. Derynck, *Molecular mechanisms of epithelial-mesenchymal transition.* Nat Rev Mol Cell Biol, 2014. **15**(3): p. 178-96.
175. Imai, K., et al., *Membrane-type matrix metalloproteinase 1 is a gelatinolytic enzyme and is secreted in a complex with tissue inhibitor of metalloproteinases 2.* Cancer Res, 1996. **56**(12): p. 2707-10.
176. Blenis, J., *Signal transduction via the MAP kinases: proceed at your own RSK.* Proc Natl Acad Sci U S A, 1993. **90**(13): p. 5889-92.
177. Murthy, S.R., et al., *Carboxypeptidase E protects hippocampal neurons during stress in male mice by up-regulating prosurvival BCL2 protein expression.* Endocrinology, 2013. **154**(9): p. 3284-93.
178. Skalka, N., et al., *Carboxypeptidase E: a negative regulator of the canonical Wnt signaling pathway.* Oncogene, 2013. **32**(23): p. 2836-47.
179. Lo Cicero, A., et al., *Microvesicles shed by oligodendroglioma cells and rheumatoid synovial fibroblasts contain aggrecanase activity.* Matrix Biol, 2012. **31**(4): p. 229-33.
180. Kahlert, U.D., G. Nikkhah, and J. Maciaczyk, *Epithelial-to-mesenchymal(-like) transition as a relevant molecular event in malignant gliomas.* Cancer letters, 2013. **331**(2): p. 131-8.
181. Chesnelong, C., Luchman, .A., Cairncross, J.G., Weiss, S. , *STAT3 is a key regulator of an "EMT-like" process mediated by Slug in GBM.* AACR Conference 2016, 2016.
182. Yang, M., et al., *L1 stimulation of human glioma cell motility correlates with FAK activation.* Journal of neuro-oncology, 2011. **105**(1): p. 27-44.

183. Kondaveeti, Y., I.K. Guttilla Reed, and B.A. White, *Epithelial-mesenchymal transition induces similar metabolic alterations in two independent breast cancer cell lines.* Cancer Lett, 2015. **364**(1): p. 44-58.
184. Joannes, A., et al., *Fhit regulates EMT targets through an EGFR/Src/ERK/Slug signaling axis in human bronchial cells.* Mol Cancer Res, 2014. **12**(5): p. 775-83.
185. Stepanenko, A.A., et al., *mTOR inhibitor temsirolimus and MEK1/2 inhibitor U0126 promote chromosomal instability and cell type-dependent phenotype changes of glioblastoma cells.* Gene, 2016. **579**(1): p. 58-68.
186. Goldberg, L. and Y. Kloog, *A Ras inhibitor tilts the balance between Rac and Rho and blocks phosphatidylinositol 3-kinase-dependent glioblastoma cell migration.* Cancer Res, 2006. **66**(24): p. 11709-17.
187. Steelman, L.S., et al., *Roles of the Ras/Raf/MEK/ERK pathway in leukemia therapy.* Leukemia, 2011. **25**(7): p. 1080-94.
188. Aguilar-Martinez, E., C. Morrisroe, and A.D. Sharrocks, *The ubiquitin ligase UBE3A dampens ERK pathway signalling in HPV E6 transformed HeLa cells.* PLoS One, 2015. **10**(3): p. e0119366.
189. Chetram, M.A. and C.V. Hinton, *PTEN regulation of ERK1/2 signaling in cancer.* J Recept Signal Transduct Res, 2012. **32**(4): p. 190-5.
190. Chung, J., et al., *STAT3 serine phosphorylation by ERK-dependent and -independent pathways negatively modulates its tyrosine phosphorylation.* Molecular and cellular biology, 1997. **17**(11): p. 6508-16.

191. Hu, B., et al., *ADP-ribosylation factor 6 regulates glioma cell invasion through the IQ-domain GTPase-activating protein 1-Rac1-mediated pathway.* Cancer Res, 2009. **69**(3): p. 794-801.
192. Verbovsek, U., et al., *Expression analysis of all protease genes reveals cathepsin K to be overexpressed in glioblastoma.* PLoS One, 2014. **9**(10): p. e111819.

9. AKNOLEDGEMENTS

Firstly, I would like to express my gratitude to my advisor Prof. Ulrike Naumann for the possibility to work in her group, the support during my Ph.D study and the writing of this thesis.

Besides my advisor, I would like to thank the rest of my advisory board committee: Prof. Feil, Prof. Maljevic, and Prof. Liebau for their insightful comments and encouragement, but also for the hard questions which gave me the chance to explore my research from various perspectives.

My sincere thanks also goes to our collaboration partners. Without their support it would not have been possible to conduct this research:

Prof. Michel Mittelbronn and Elena I. Ilina from the Institute of Neurology (Edinger Institute), Goethe University, Frankfurt am Main, Germany.

Prof. Laurent Vallar, Tony Kaoma, Arnaud Muller from the Genomics and Proteomics Research Unit, Department of Oncology, Luxembourg Institute of Health (L.I.H.) Luxembourg.

Prof. Simone Niclou from the NORLUX Neuro-Oncology Laboratory, Luxembourg Institute of Health, Luxembourg.

Prof. Marcel Krüger from the Department of Preclinical Imaging and Radiopharmacy, University of Tübingen, Germany.